# Photonic Pulse Shaping Techniques for Arbitrary Waveform Generation

Pablo I. Palacios Tomás

Under supervision of María C. Santos Blanco

Submitted in partial satisfaction of the requirements for the
degree of

Engineering Physics Bachelor's Thesis

Escola Tècnica Superior de Enginyeria de Telecomunicacions de Barcelona

Universitat Politècnica de Catalunya

June, 2021

# Abstract

The motivation of this thesis is to explore the generation of arbitrary microwave waveforms through photonic means, showing the advantages they may offer. Some techniques will be presented for this purpose, as well as their applications.

Firstly, the technique known as Direct Space To Time Mapping (DST) will be presented, which as the name properly says, turns the spatial profile into the time profile of the beam.

Then, we will present the main technique of the thesis, which shows a great analogy with the DST. This technique is known as Frequency to Time Mapping (FTM) or Direct Fourier Transformation (DFT). In order to derive the expressions needed for the understanding of the DFT, dispersion theory in media will be explained starting from the macroscopic Maxwell equations derived in the appendix.

It will be seen how combining spectrum shaping techniques along with the DFT we are able to generate an arbitrary radio-frequency waveform. After being mathematically derived, simulations will be performed to put numbers and further prove of the theory. The achievable time bandwidth product (TBWP) will also be derived and later compared to the one obtained by Matlab simulation.

Furthermore, the DFT will then be applied for time reversal by photonic means. A microwave signal up to 10 nanoseconds long can be time-reversed using fibers, as it will be proved in theory and simulation.

Applications related to these microwave generation techniques will also be explored, showing the research interest of this cutting-edge discipline.

# Table of Contents

# List of Figures

# Chapter 1

# Introduction

Microwave Photonics (Capmany and Novak, 2007) (Jäger and Stöhr, 2005) is currently a very active research field, combining the potential of photonics techniques and technologies for the processing of microwave (MW) signals, involving either the generation, manipulation, transport or measurement of radio frequency (RF) signals.

The scope of this thesis is to show and explain pulse shaping techniques which allow the generation of arbitrary microwave signals, as well as the applications they may have, pointing out the benefits with respect to other electronic technologies present in the industry nowadays. Needless to say, RF signals are currently one of the most important means of communication and of vast applications in many other fields, and hence, the possibility of modeling them with precision is of very high interest. Recent works have also expanded the range of the generated waves to the THz regime (Veli et al., 2021).

The presented techniques can provide signals with very high values of time-bandwidth product (TBWP) (C. Wang, 2014) useful for many current applications such as ultrawide-band and multiple-access communications systems (R. Qiu, Liu and Shen, 2005), electronic countermeasures, high-penetration and high-precision radars (Pan and Y. Zhang, 2020), medical imaging and modern instrumentation systems (Hämäläinen et al., 2021), which cannot be achieved by electronic means (C. Wang, Hao Chi and Jianping Yao, 2008) (Jianping Yao, 2011) as digital electronics are limited to lower frequencies and bandwidth. Photonic tecniques are better suited to perform real

time high-speed processing and measurements. As a counterpart, photonic systems may be costly and harder to implement.

A set of photonic techniques for microwave generation (MWG) are hence presented, proved and discussed in this thesis aiming to advance in understanding and development of such cutting-edge techniques.

The first technique to be presented is Direct Space To Time Mapping (DST), which turns the spatial profile of the outgoing laser into the time profile of the signal. This technique makes use of lenses and gratings. Compared to the following techniques, this one presents the problem of propagation in free-space, which makes the system bulky and costly, as well as hard to calibrate.

The Direct Fourier Transformation (DFT) or Frequency to Time Mapping (FTM) is then presented, which combined with spectrum shaping can generate arbitrary radio-frequency waveforms, showing a TBWP not reachable by other means. Recent works have shown that through little add-ups to this technique (Rashidinejad and A. M. Weiner, 2014) a TBWP equal to the upper bound given by the number of pulse shaper control elements can be obtained, which is ultimately given by the resolution and range of the waveshaper.

The achievable TBWP by the latter will also be derived and later compared to the one obtained by Matlab simulation.

Making use of the DFT, a method for time reversal of a RF signal through photonics will be performed. Time reversal (TR) has been proved to have many applications, specially in transmission of ultrawide-band signals (which can be reached through the explained methods) in wireless communication for rich multipath environments (R. Qiu, Liu and Shen, 2005) (Alexandropoulos et al., 2019).

Other applications related to these microwave generation techniques will as well be explored.

# Chapter 2

# Theoretical basis

In this chapter we present the dispersion theory needed for the purpose of reaching the goals of the thesis. First of all, for clarification and unification in criteria we shall define Fourier transforms for time and space, which are needed for the subsequent explanations. Then, starting from the Maxwell macroscopic equations, presented in the Appendix A, the transfer function in dispersive media is derived, in the frequency and in the time domain. Finally, the TBWP is both defined and explained.

## 2.1   Fourier Transform Criterion

Here we present the Fourier transform criterion we have chosen to be used during the thesis. The first two expressions correspond to time to frequency and frequency to time transformations while the last two relate space to spatial frequency and vice versa.

$$F(w) = \mathscr{F}\{f(t)\}(w) = \int_{-\infty}^{\infty} f(t)e^{-jwt}dt. \tag{2.1}$$

$$f(t) = \mathscr{F}^{-1}\{F(w)\}(t) = \frac{1}{2\pi}\int_{-\infty}^{\infty} F(w)e^{jwt}dw. \tag{2.2}$$

$$S(k) = \mathscr{F}\{s(x)\}(k) = \int_{-\infty}^{\infty} s(x)e^{jkx}dx. \tag{2.3}$$

$$s(x) = \mathscr{F}^{-1}\{S(k)\}(x) = \frac{1}{2\pi}\int_{-\infty}^{\infty} S(k)e^{-jkx}dk. \tag{2.4}$$

## 2.1.1 Dispersion in media

Starting from the standard macroscopic Maxwell equations derived in the appendix, we can obtain for the electric ($\mathbf{E}$) and magnetic fields ($\mathbf{H}$) the following relation:

$$\nabla \times (\nabla \times \mathbf{E}) = -\nabla \times \frac{\partial \mathbf{B}}{\partial t}. \tag{2.5}$$

Substituting $\mathbf{B}$ by its correspondence with the fields $\mathbf{H}$ and $\mathbf{M}$ (A.10) we arrive to:

$$\nabla \times (\nabla \times \mathbf{E}) = -\nabla \times \mu_0 \frac{\partial (\mathbf{H} + \mathbf{M})}{\partial t}. \tag{2.6}$$

Doing the proper for $\mathbf{H}$ and its relation with $\mathbf{D}$ and $\mathbf{J}_{free}$ (A.12),

$$\nabla \times (\nabla \times \mathbf{E}) = -\mu_0 \frac{\partial^2 \mathbf{D}}{\partial t^2} - \mu_o \frac{\partial \mathbf{J}_{free}}{\partial t} - \nabla \times \mu_0 \frac{\partial \mathbf{M}}{\partial t}. \tag{2.7}$$

Now we assume an isotropic, sourceless, homogeneous, non magnetic and non conductive medium. Therefore, the equation can be simplified:

$$\nabla^2 \mathbf{E} = \mu_0 \epsilon_0 \frac{\partial^2 \mathbf{E}}{\partial t^2} + \mu_0 \frac{\partial^2 \mathbf{P}}{\partial t^2}, \tag{2.8}$$

where we have been able to perform such simplifications taking into account that the medium meets all the requirements previously mentioned. Expressing the latter in Cartesian coordinates reads:

$$\left( \frac{\partial^2}{\partial x^2} + \frac{\partial^2}{\partial y^2} + \frac{\partial^2}{\partial z^2} - \frac{1}{c^2} \frac{\partial^2}{\partial t^2} \right) \mathbf{E} = -\mu_0 \frac{\partial^2 \mathbf{P}}{\partial t^2}, \tag{2.9}$$

taking into account that $c = \frac{1}{\sqrt{\epsilon_0 \mu_0}}$, where c is the speed of light in vacuum.

The response of the medium is hence given by the polarization $\mathbf{P}$. Usually this polarization is decomposed into two terms, the linear term and the non-linear one, $\mathbf{P} = \mathbf{P}_L + \mathbf{P}_{NL}$. We will only consider the linear effects here, as we are staying in the frame of linear optics.

As known from classical electrodynamics (Jackson, 1975) when the linear polarization is parallel to the electric field the medium is said to be isotropic, the proportionality

coefficient will not depend on the direction, but it may depend on the frequency. In the frequency domain we have:

$$\tilde{\mathbf{P}}_L(w,z) = \epsilon_0 \chi(w)\tilde{\mathbf{E}}(w,z), \tag{2.10}$$

where $\chi(w)$ is the frequency-dependent term called electric susceptibility. The tilde shows the complex nature of the electric field in the frequency domain. The dielectric constant is expressed as a function of the previous as:

$$\epsilon(w) = \Big(1 + \chi(w)\Big)\epsilon_0. \tag{2.11}$$

As a function of time, using the convolution theorem:

$$\mathbf{P}_L(t,z) = \int_{-\infty}^{t} \epsilon_0 \chi(t')\mathbf{E}(t-t',z)dt', \tag{2.12}$$

where the upper limit is $t$, expressing the causal response of the medium.

Going back to equation (2.9) some simplifications are made to allow the equation to be resolved. First of all we suppose that the wave propagates in the $z$ direction. Hence, it can be assumed that the variations in the $x$ and $y$ directions are negligible in comparison to the ones in the $z$ direction (paraxial regime).

Thus, the equation is reduced to:

$$\left(\frac{\partial^2}{\partial z^2} - \frac{1}{c^2}\frac{\partial^2}{\partial t^2}\right)\mathbf{E}(t,z) = -\mu_0 \frac{\partial^2 \mathbf{P}(t,z)}{\partial t^2}, \tag{2.13}$$

obviating the dependence on $x$ and $y$.

Furthermore, the Fourier transform of the latter along with expressions (2.10) and (2.11) gives place to:

$$\left(\frac{\partial^2}{\partial z^2} + \frac{1}{c^2}w^2\right)\tilde{\mathbf{E}}(w,z) = -\mu_0 \epsilon_0 w^2 \chi(w)\tilde{\mathbf{E}}(w,z) \tag{2.14}$$

$$\left(\frac{\partial^2}{\partial z^2} + w^2 \mu_0 \epsilon(w)\right)\tilde{\mathbf{E}}(w,z) = 0, \tag{2.15}$$

getting to the final wave equation. The general solution for the latter is:

$$\tilde{E}(w, z) = K_1 e^{-jk(w)z} + K_2 e^{jk(w)z} \tag{2.16}$$

$$K_1 + K_2 = \tilde{E}(w, 0). \tag{2.17}$$

Taking the solution propagating in the positive direction:

$$\tilde{E}(w, z) = \tilde{E}(w, 0)e^{-jk(w)z}, \tag{2.18}$$

where $k$ is defined by the dispersion relation:

$$k^2(w) = w^2 \mu_0 \epsilon(w) = \frac{w^2}{c^2}\left(1 + \chi(w)\right) = \frac{w^2}{c^2}n^2(w), \tag{2.19}$$

where $n(w)$ is the refractive index of the material. The bandwidth $\tilde{w} = w - w_0$ is much smaller than the carrier frequency $w_0$. So we can expand $k(w)$ around the carrier frequency $w_0$:

$$k(w) = k(w_0) + \frac{dk}{dw}\bigg|_{w_0}(w - w_0) + \frac{d^2k}{dw^2}\bigg|_{w_0}(w - w_0)^2 + O(w^3). \tag{2.20}$$

We can neglect higher order terms and equation (2.18) can be rewritten as:

$$\tilde{E}(w, z) = \tilde{E}(w, z)e^{-jk_0 z}e^{-j\delta k z} \tag{2.21}$$

Where $k_0$ is $k(w_0)$ and $\delta k = k(w) - k_0$. The free-space wavenumber $k_0$ has to be much higher than $\delta k$, so the field variations over distances of the order of the wavelength are much smaller than the value of the envelope itself (Slowly Varying Envelope Approximation, SVEA, in space). Then it makes sense to represent the envelope of the previous pulse as centered at $w_0$:

$$\tilde{\mathcal{E}}(w, z) = \tilde{E}(w + w_0, t)e^{-j\delta k z} \tag{2.22}$$

This is a pure mathematical expression and all waves can be represented like this, however it does not make sense for all waves to be represented by an envelope and a carrier frequency if the following equation for the SVEA is not satisfied:

$$\left| \frac{\partial}{\partial z} \tilde{\mathcal{E}}(w, z) \right| \ll k_0 |\tilde{\mathcal{E}}(w, z)| \qquad (2.23)$$

Leading to:

$$\left| \frac{\delta k}{k_0} \right| \ll 1 \qquad (2.24)$$

Meaning that the envelope does not change significantly after traveling a distance of the order of the carrier wavelength $\lambda_0 = \frac{2\pi}{w_0}$.

Performing the Fourier transform on (2.21):

$$\tilde{E}(t, z) = \left[ \frac{1}{2\pi} \int_{\infty}^{\infty} dw \tilde{E}(w, z) e^{-j\delta k z} e^{j(w - w_0)t} \right] e^{j(w_0 t - k_0 z)} \qquad (2.25)$$

Which can be expressed as:

$$\tilde{E}(t, z) = \tilde{\mathcal{E}}(t, z) e^{j(w_0 t - k_0 z)} \qquad (2.26)$$

Where $\tilde{\mathcal{E}}(t, z)$ is now the time envelope of the pulse, corresponding to the integral inside the brackets. For simplification of nomenclature, from now on, we will obviate the tilde that represents the complex nature of the field/envelope.

Further simplification of the wave equation requires the use of some envelope properties. First of all, we expand $\epsilon(w)$ around $w_0$, taking into account equations (2.10) and (2.11), it leads to the following expression for the linear polarization:

$$\mathbf{P}_L(w, z) = \left( \epsilon(w_0) - \epsilon_0 + \sum_{n=1}^{\infty} \frac{d^n \epsilon}{dw^n} \bigg|_{w_0} (w - w_0)^n) \right) \mathbf{E}(w, z). \qquad (2.27)$$

Expressing it in terms of the time pulse envelope:

$$\mathbf{P}_L(t, z) = \left[ \left( \epsilon(w_0) - \epsilon_0 \right) \mathcal{E}(t, z) + \sum_{n=1}^{\infty} (-j)^n \frac{d^n \epsilon}{dw^n} \bigg|_{w_0} \frac{\partial^n}{\partial t^n} \mathcal{E}(t, z) \right] e^{j(w_0 t - k_0 z)}, \qquad (2.28)$$

where the term inside the brackets describes the slowly time varying envelope of the polarization vector.

The next step is to change the coordinate system, adopting the retarded frame of

reference, moving with the group velocity $v_g = \left( \left. \frac{dk}{dw} \right|_{w_0} \right)^{-1}$. Therefore, the following transformations are performed:

$$\zeta = z, \qquad\qquad\qquad \vartheta = t - \frac{z}{v_g}, \qquad\qquad (2.29)$$

and according to the chain rule:

$$\frac{\partial}{\partial z} = \frac{\partial}{\partial \zeta} - \frac{1}{v_g}\frac{\partial}{\partial \vartheta}, \qquad\qquad\qquad \frac{\partial}{\partial t} = \frac{\partial}{\partial \vartheta}. \qquad\qquad (2.30)$$

When performing calculations on (2.13) using (2.25) and (2.28) in the new coordinate system we obtain (Diels and Rudolph, 2006):

$$\frac{\partial}{\partial \zeta}\mathcal{E}(\vartheta,\zeta) - \frac{j}{2}k_0''\frac{\partial^2}{\partial \vartheta^2}\mathcal{E}(\vartheta,\zeta) + \Theta = \frac{-j}{2k_0}\frac{\partial}{\partial \zeta}\left(\frac{\partial}{\partial \zeta} - \frac{2}{v_g}\frac{\partial}{\partial \vartheta}\right)\mathcal{E}(\vartheta,\zeta), \qquad (2.31)$$

where $\Theta$ represents the higher order terms.

It can also be observed that the second derivative of $k$ centered at $w_0$ comes out in the equation. By strict derivation this factor is expressed as:

$$k_0'' = \left. \frac{d^2k}{dw^2} \right|_{w_0} = -\frac{1}{v_g^2}\left. \frac{dv_g}{dw} \right|_{w_0} = GVD. \qquad\qquad (2.32)$$

This second derivative is mostly known as the group velocity dispersion (GVD) parameter. In order to simplify the wave equation we have to take into account some of the properties previously described for these pulses and their envelopes.

We first present the SVEA in the time domain, which is quite similar to the one in space, i.e.:

$$\left| \frac{\partial}{\partial t}\mathcal{E}(t,z) \right| \ll w_0|\mathcal{E}(t,z)|. \qquad\qquad (2.33)$$

The right hand side term in (2.31) can be neglected according to (2.23) (Sazonov, 2017) along with the SVEA in time (2.33), as seen below, where the dependency of the coordinates for the envelope has been omitted:

$$\frac{-j}{2k_0}\frac{\partial}{\partial\zeta}\left(\frac{\partial}{\partial\zeta}-\frac{2}{v_g}\frac{\partial}{\partial\vartheta}\right)\mathcal{E}=\frac{-j}{2k_0}\frac{\partial}{\partial\zeta}\left(\frac{\partial}{\partial z}-\frac{1}{v_g}\frac{\partial}{\partial t}\right)\mathcal{E},\tag{2.34}$$

$$\left|\frac{-j}{2k_0}\left(\frac{\partial}{\partial z}-\frac{1}{v_g}\frac{\partial}{\partial t}\right)\mathcal{E}\right|\ll|\mathcal{E}|.\tag{2.35}$$

Thus:

$$\left|\frac{-j}{2k_0}\frac{\partial}{\partial\zeta}\left(\frac{\partial}{\partial\zeta}-\frac{2}{v_g}\frac{\partial}{\partial\vartheta}\right)\mathcal{E}\right|\ll\left|\frac{\partial}{\partial\zeta}\mathcal{E}\right|.\tag{2.36}$$

Having proved the latter, we can now neglect the right hand side term of equation (2.31). For even further simplifications, the higher order polarization terms can also be omitted, therefore $\Theta=0$, this is the case of a dielectric constant changing slowly over frequencies within the pulse spectrum. If so, equation (2.31) reduces to:

$$\frac{\partial}{\partial\zeta}\mathcal{E}(\vartheta,\zeta)-\frac{j}{2}k_0''\frac{\partial^2}{\partial\vartheta^2}\mathcal{E}(\vartheta,\zeta)\simeq0.\tag{2.37}$$

Assuming the new frame of reference moving with the group velocity, from now on, the $\vartheta$ will be substituted by $t$ and the $\zeta$ by $z$. Equation (2.37) may be solved in the frequency domain. Therefore we express the field envelope in the time domain as the inverse Fourier transform of the electric field envelope as a function of the frequency:

$$\mathcal{E}(z,t)=\frac{1}{2\pi}\int_{-\infty}^{\infty}\mathcal{E}(w,z)e^{jwt}dw,\tag{2.38}$$

then, we substitute the subsequent expression in equation (2.37), giving place to:

$$\frac{1}{2\pi}\int_{-\infty}^{\infty}\left[\frac{\partial\mathcal{E}}{\partial z}+j\frac{k_0''w^2}{2}\mathcal{E}\right]e^{jwt}dw=0,\tag{2.39}$$

which is fulfilled when:

$$\frac{\partial\mathcal{E}}{\partial z}+j\frac{k_0''w^2}{2}\mathcal{E}=0,\tag{2.40}$$

with solution:

$$\mathcal{E}(w,z)=\mathcal{E}(w,0)e^{-j\frac{w^2k_0''}{2}z},\tag{2.41}$$

clearly seeing the effect of the dispersion and identifying it with the following transfer function:

$$H(w, z) = e^{-j\frac{w^2 k_0''}{2}z}. \tag{2.42}$$

Hence, according to the theory for linear time invariant systems, in the time domain the effect of the dispersion is expressed as the convolution between the pulse and the impulse response function:

$$\mathcal{E}(t, z) = h(t, z) * \mathcal{E}(t, 0) = \int_{-\infty}^{\infty} h(t - t', z)\mathcal{E}(t', 0)dt'. \tag{2.43}$$

In order to find the expression for the impulse response function, it is only needed to perform the inverse Fourier transform to the transfer function:

$$h(t, z) = \frac{1}{2\pi} \int_{-\infty}^{\infty} H(w, z)e^{jwt}dw, \tag{2.44}$$

$$h(t, z) = \frac{e^{\frac{j}{2k_0'' z}t^2}}{\sqrt{j2\pi k_0'' z}}. \tag{2.45}$$

From now on the factor $k''z$ will be substituted by the letter $\Theta$ as these two parameters come always multiplying and hence, expressions become clearer. This parameter is commonly known as group delay dispersion (GDD).

$$GDD = GVD \cdot z = \left.\frac{d^2 k}{dw^2}\right|_{w_0} \cdot z \tag{2.46}$$

Sometimes, the dispersion value is not given by the GDD. It is usual in literature and in the industry to give the dispersion value as the delay dispersion coefficient, defined by the derivative of the inverse of the velocity group with respect to wavelength (rather than angular frequency).

$$D(\lambda) = \frac{\partial}{\partial\lambda}\frac{1}{v_g} \tag{2.47}$$

Taking into account that $w = \frac{2\pi c}{\lambda}$, the GVD and the dispersion coefficient are related by:

$$D = \frac{\partial}{\partial\lambda}\frac{1}{v_g} = \frac{\partial}{\partial\lambda}\frac{\partial k}{\partial w} = \frac{\partial w}{\partial\lambda}\frac{\partial}{\partial w}\frac{\partial k}{\partial w} = \frac{-2\pi c}{\lambda^2}\frac{\partial^2 k}{\partial w^2} = \frac{-2\pi c}{\lambda^2}GVD \tag{2.48}$$

Having the GVD, the total GDD is easily found multiplying by the length of the fiber.

## 2.1.2 The case of the Gaussian pulse

For the case of the Gaussian pulse dispersion, an analytical solution can be found. The Gaussian pulse may be expressed as (Ladányi, Menkyna and Mullerova, 2013):

$$\mathcal{E}(t,0) = \mathcal{E}_0 e^{-(\frac{t}{\tau_0})^2}, \tag{2.49}$$

working in the frequency domain, the expression for the output is:

$$\mathcal{E}(t,z) = \int_{-\infty}^{\infty} \mathcal{E}(w,0)e^{-j\frac{\Theta}{2}w^2}e^{jwt}dw, \tag{2.50}$$

where $\mathcal{E}(w,0)$ comes given by the Fourier transform:

$$\mathcal{E}(w,0) = \frac{1}{2\pi}\int_{-\infty}^{\infty} e^{-(\frac{t}{\tau_0})^2}e^{-jwt}dt = \mathcal{E}_0\sqrt{\pi}\tau_0 e^{-\frac{w^2\tau_0^2}{4}}. \tag{2.51}$$

Substituting the latter in (2.50):

$$\mathcal{E}(t,z) = \frac{\mathcal{E}_0\sqrt{\pi}\tau_0}{2\pi}\int_{-\infty}^{\infty} e^{-\frac{w^2\tau_0^2}{4}}e^{-j\frac{\Theta}{2}w^2}e^{jwt}dw, \tag{2.52}$$

$$\mathcal{E}(t,z) = \frac{\mathcal{E}_0\tau_0}{2}\frac{1}{\left(\frac{\tau_0^2}{4}+j\frac{\Theta}{2}\right)^{\frac{1}{2}}}e^{-\frac{t^2}{\tau_0^2+2j\Theta}}. \tag{2.53}$$

The Gaussian pulse, although maintaining its Gaussian shape through propagation, is broadened and acquires a phase chirp. A chirp is the temporal variation of the phase around the carrier frequency $w_0$. The field can be expressed as $E(t) = |E_0|e^{\psi(t)}$, with $\psi(t) = \phi_0 + \phi(t)$.

The instantaneous frequency of the total pulse is given by:

$$w_{inst}(t) = w_0 + \frac{d}{dt}\phi(t). \tag{2.54}$$

If it is linearly time-dependent, then we say the pulse is chirped or frequently modulated:

$$w_{inst}(t) = w_0 + \alpha t, \tag{2.55}$$

where $\alpha$ is the chirp parameter. When we talk in terms of the pulse envelope, this carrier frequency is omitted as shown in (2.26). In order to see the chirp and broadening of the pulse we can rewrite expression (2.53) as:

$$\mathcal{E}(t,z) = \frac{\mathcal{E}_0 \tau_0}{2} \frac{1}{\left(\frac{\tau_0^2}{4} + j\frac{\Theta}{2}\right)^{\frac{1}{2}}} e^{-\left(\frac{t^2}{\tau_0^2 + \frac{4\Theta^2}{\tau_0^2}}\right)} e^{j\left(\frac{2t^2}{\frac{\tau_0^4}{\Theta} + 4\Theta}\right)},$$ 
<div align="right">(2.56)</div>

where we can clearly see the time broadening in the first exponential by a factor $M = \sqrt{1 + 4\Theta^2/\tau_0^4}$ and a chirp parameter $\alpha = \frac{1}{\frac{\tau_0^4}{4\Theta} + \Theta}$.

## 2.2   Time-Bandwidth product

The time-bandwidth product (TBWP) is a parameter that describes the relation between the time duration of the pulse and its bandwidth. Both the concepts of time duration and bandwidth entail a certain degree of arbitrariness, as it is difficult to precisely define where a function starts and ends, since it cannot be limited in time and bandwidth all at once. A parameter commonly used in the literature (Papoulis, 1977) to define the time duration $\Delta t$, specially in Gaussian pulses, is the full width at half maximum (FWHM) of the intensity profile, related to the absolute square value of the field $|\mathcal{E}(t)|^2$. Mathematically this reads as $|\mathcal{E}(\frac{\Delta t}{2})|^2 = \frac{\mathcal{E}^2(t=0)}{2} = \frac{\mathcal{E}_0^2}{2}$. For the bandwidth, the same procedure is followed, taking the FWHM of the spectral intensity $|\mathcal{E}(w)|^2$, now derived from $|\mathcal{E}(\frac{\Delta w}{2})|^2 = \frac{|\mathcal{E}(w=0)|^2}{2}$. There are other ways of defining the time duration and bandwidth, however this is the most common and the one we will employ. These definitions will only have meaning if the pulse's time and frequency profile follow a well-defined decaying trend.

Since the time duration and the bandwidth are related by Fourier transformation, the inequality derived from the uncertainty principle for Fourier transform pairs gives place to:

$$TBWP = \Delta w \Delta t \geq c$$
<div align="right">(2.57)</div>

Where c is a constant that depends on the pulse shape and is of the order of $2\pi$.

The equality holds for what are called Transform-limited pulses, usually understood as the pulse with the lowest time duration achievable for a given spectrum. The condition of being at the transform limit is essentially equivalent to the condition of a frequency-independent spectral phase, basically implying that the time–bandwidth product is at its minimum and that there is no chirp, as it is the case of the non-chirped Gaussian pulse.

Since we are interested in Gaussian pulses, produced by Mode-Locked Lasers (MLL), we will analyze them, looking for the value of c and how the TBWP changes through propagation in a dispersive media. As seen in section 2.1.2, the pulse envelope is expressed as a function of time as:

$$\mathcal{E}(t) = \mathcal{E}_0 e^{-(\frac{t}{\tau_0})^2} \tag{2.58}$$

and as a function of the frequency:

$$\mathcal{E}(w) = \mathcal{E}_0 \sqrt{\pi} \tau_0 e^{-\frac{w^2 \tau_0^2}{4}}. \tag{2.59}$$

Hence, the FWHM for time and bandwidth are:

$$\Delta t = \tau_0 \sqrt{2ln2}, \tag{2.60}$$

$$\Delta w = \frac{2\sqrt{2ln2}}{\tau_0}. \tag{2.61}$$

Therefore the TBWP will be:

$$TBWP = 4 \cdot ln2 \simeq 2.77, \tag{2.62}$$

which suggests that the product only depends on the kind of pulse (Gaussian, Lorentzian, squared...) but not on parameters such as the temporal length. However, after going through a dispersive propagation the pulse changes the TBWP, becoming bigger (the only possible way, as stated by (2.57)). The pulse is broadened in time, as seen in (2.56) and mentioned in the end of section 2.1.2, while the modulus of the spectrum remains constant (only a phase shift is introduced by dispersion).

There is another definition for the bandwidth that will often be used during the

thesis because it offers some simplifications and it may sometimes be more visual. Because of the properties of Fourier transformations, it is seen straightforwardly that the bandwidth of a Gaussian pulse in Hz is inversely proportional to the time duration (2.61) (directly related to $\tau_0$ (2.60)), so $BW \propto \frac{1}{\tau_0}$, or in radians $\frac{2\pi}{\tau_0}$. When substituting the $\Delta w$ by $\Delta w_{Tot} = \frac{2\pi}{\tau_0}$ we see that this value is the Full Width at 0.0848 Maximum, almost equivalent to the bandwidth at $-10\ dB$, comprising most of the spectral intensity, understanding it as a more extended estimation of the bandwidth. As we will use the Full Width at $\sim -10\ dB$ Maximum for the "total" bandwidth, we might as well use it when talking about the estimated "total" time duration or the estimated "total" beam width.

In the case of a Gaussian function $e^{-(\frac{x}{x_0})^2}$, the Full Width at approximately $-10\ dB$ is:

$$\Delta x = \frac{\pi}{\sqrt{2}} x_0 \tag{2.63}$$

# Chapter 3

# Techniques

## 3.1 Pulse Shaping Techniques

### 3.1.1 Direct Space to Time Transformation

First of all we will present a technique based on diffraction without any use of dispersion. In order to do that, the system gratings ought to be dispersion-free (Treacy, 1969), this system is of particular interest since there is an analogy with the system that will be presented later (DFT). The set-up used for this transformation is shown in Figure 3.1.



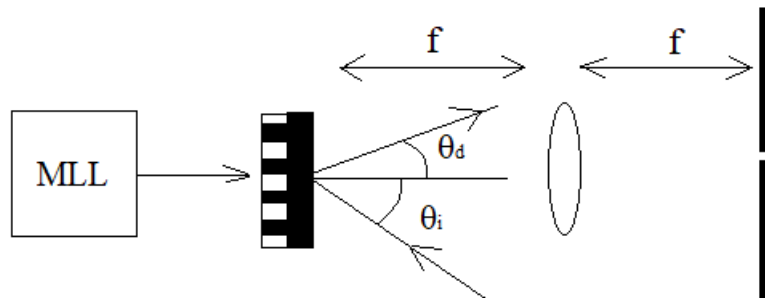Figure 3.1: Set-up used for Direct Space to Time (DST). Consisting on a Mode-Locked Laser (MLL), a mask $m(x)$, a diffraction grating, a lens separated from it a distance equal to the focal length and a very small slit at the back focal plane.

We begin with an ultra-short pulse with a spatial profile $s(x)$ and a time profile $a(t)$. Later on, the expressions will be particularized for a Gaussian pulse, but for now

we will keep it general. The central frequency of the pulse will be $w_0$, so it can be expressed as:

$$E_{in}(x,t) = Re[\mathcal{E}_{in}(x,t)e^{jw_0 t}] = Re[s(x)a(t)e^{jw_0 t}]. \tag{3.1}$$

Then the pulse goes through a grating, which, basically, angularly disperses the different frequency components contained within the incident pulse. We will not go into a deep explanation of the behavior of the grating, the output expression, assuming paraxial propagation, is shown below ('Manipulation of Ultrashort Pulses' 2009):

$$E_2(x,t) = \sqrt{\beta_a} Re[\int \frac{d\tilde{w}}{2\pi} A(\tilde{w})s(\beta_a x)e^{-j\gamma\tilde{w}x}e^{j(\tilde{w}+w_0)t}] \tag{3.2}$$

being:

$$\tilde{w} = w - w_0 \qquad\qquad \beta_a = \frac{cos(\theta_i)}{cos(\theta_d)} \qquad\qquad \gamma = \frac{2\pi}{w_0 d cos(\theta_d)} \tag{3.3}$$

where $\theta_i$ is the angle of a reference incident ray, $\theta_d$ the reference ray diffraction angle, $d$ is the periodicity of the grating rulings and $A(w)$ is the Fourier transform of $a(t)$. We have considered here a diffraction order equal to -1.

Following this last step, the pulse now goes through a lens separated from the grating by a distance equal to the focal length,.

According to the popular Fresnel's equation, in the focal plane after the lens we obtain the Fourier transform of the incoming spatial profile, converting the angular dispersion performed by the grating into a spatial one in the back focal plane.

If we consider the effect of diffraction and the lens for a monochromatic field, in the paraxial regime, with slow variations in space when compared to the wavelength scale, the initial spatial profile in 1D and taking therefore into account that $k = 2\pi/\lambda$; for a signal $s(x)$ the spatial profile of the field previously described at back focal plane is given by:

$$s_{out}(x) = \sqrt{\frac{j}{\lambda f}} \int_{\infty}^{\infty} s(x) e^{jkxx'/f} dx' = \sqrt{\frac{j}{\lambda f}} S(\frac{kx}{f}) \qquad (3.4)$$

Thus, if we we apply this expression along with the equation (3.2) we obtain the next equation for the field at the lens focal plane:

$$E_{out}(x,t) = Re\left[\sqrt{\frac{j\beta_a}{\lambda f}} \int_{-\infty}^{\infty} \frac{1}{2\pi} A(\tilde{w}) e^{j(w_0+\tilde{w})t} \left(\int_{-\infty}^{\infty} s(\beta_a x') e^{-j\tilde{w}\gamma x'} e^{j\frac{kxx'}{f}} dx'\right) d\tilde{w}\right],$$
$$(3.5)$$

following the usual notation of $S(k)$ as the Fourier transform of s(x):

$$E_{out}(x,t) = Re\left[\int_{-\infty}^{\infty} \frac{1}{2\pi} \sqrt{\frac{j}{\lambda f \beta_a}} A(\tilde{w}) e^{j(w_0+\tilde{w})t} S\left(\left(\frac{kx}{f} - \gamma\tilde{w}\right)\frac{1}{\beta_a}\right) d\tilde{w}\right], \qquad (3.6)$$

which is a multiplication in the frequency domain of the Fourier transform of the spatial profile (the frequency profile of the input pulse) and a rescaled version of the Fourier transform of the input pulse, with different displacement depending on the evaluated position $x$. This is called the Direct Space to Time transformation, from now on DST (D.E. Leaird and A. Weiner, 2001). As it will be seen later, this technique presents high analogy with the DFT (Dispersive Fourier Transformation).

For simplification, we will now only take into account $\mathcal{E}(x,t)$, directly related to the field by expression (3.1), therefore:

$$\mathcal{E}(x,t) = \int_{-\infty}^{\infty} \frac{1}{2\pi} \sqrt{\frac{j}{\lambda f \beta_a}} A(\tilde{w}) S\left(\left(\frac{kx}{f} - \gamma\tilde{w}\right)\frac{1}{\beta_a}\right) e^{j\tilde{w}t} d\tilde{w}. \qquad (3.7)$$

If we now place a delta slit in $x = 0$ the time profile of the envelope will come given by:

$$\mathcal{E}_{out}(t) = \sqrt{\frac{j}{\lambda f \beta_a}} \frac{1}{2\pi} \int_{-\infty}^{\infty} A(\tilde{w}) S\left(\frac{-\gamma\tilde{w}}{\beta_a}\right) e^{j\tilde{w}t} d\tilde{w}, \qquad (3.8)$$

or going back to time domain:

$$\mathcal{E}_{out}(t) = \sqrt{\frac{j\beta_a}{\lambda f}} a(t) * s\left(\frac{\beta_a t}{\gamma}\right) \tag{3.9}$$

This yields an important result, meaning that the output in time will be equal to the spatial profile in the input, scaled by a factor $\frac{\gamma}{\beta_a}$. Hence, if $a(t)$ is short enough to be considered a delta function when compared to $s\left(\frac{\beta_a t}{\gamma}\right)$, the time profile will be given by the spatial profile of the incoming pulse, and therefore controlling it, as it can be done by placing a mask or a spatial light modulator (SLM), we can control the field at the output. We shall later give numbers in order for this approximation to be valid.

Now, if the delta slit is not placed at $x = 0$ but at $x'$. Then, from equation (3.6):

$$\mathcal{E}(x,t) = \int_{-\infty}^{\infty} \frac{1}{2\pi} \sqrt{\frac{j}{\lambda f \beta_a}} A(\tilde{w}) S\left(\left(\frac{kx'}{f\gamma} - \tilde{w}\right)\frac{\gamma}{\beta_a}\right) e^{j\tilde{w}t} d\tilde{w} \tag{3.10}$$

Which only shifts the optical frequency of the filter, changing now the central frequency for the spectral response to $\tilde{w}' = \frac{kx'}{f\gamma}$. However, the shape of the outcoming pulse will not change, as only the amplitudes will do according to the spectrum of $A(\tilde{w})$ for the centered frequency modulated by the position of the slit. Once again, and for further clarification, in the time domain the field is expressed as:

$$\mathcal{E}(t)_{out} = \sqrt{\frac{j}{\lambda f \beta_a}} a(t) * \left\{ s\left(\frac{\beta_a t}{\gamma}\right) e^{j\frac{kx'}{f\gamma}} \right\} \tag{3.11}$$

Where it is seen that the system response does not change depending on the position of the slit but for a frequency shift.

E.g. we suppose an input pulse with a Gaussian temporal profile and also a spatial profile multiplied by a mask $m(x)$. For simplification we will place the slit at $x' = 0$. I.e.:

$$\mathcal{E}_{in}(x,t) = e^{-\left(\frac{t}{\tau_0}\right)^2} e^{-\left(\frac{x}{x_0}\right)^2} m(x) \tag{3.12}$$

At the output, according to (3.11):

$$\mathcal{E}_{out}(t) = \sqrt{\frac{j}{\lambda f \beta_a}} e^{-(\frac{t}{\tau_0})^2} * \{e^{-(\frac{\beta_a t}{x_0 \gamma})^2} m\left(\frac{\beta_a t}{\gamma}\right)\} \qquad (3.13)$$

Now, we can suppose the mask to cover almost the whole beam width of the laser, $\Delta x_{tot} = \frac{\pi}{\sqrt{2}} x_0$ (Full Width $\sim -10\,dB$ , as specified in (2.63)) and to have a resolution of $\delta x$. Therefore, we have approximately:

$$\Delta x_{mask} = N\delta x \simeq \frac{\pi}{\sqrt{2}} x_0 \qquad (3.14)$$

Where $\Delta x_{mask}$ is the length of the mask and N is the total number of resolution elements $\delta x$.

In order for the outcoming field to be a scaled version of the input spatial profile, the duration of the input pulse $e^{-(\frac{t}{\tau_0})^2}$, with Full Width at $-10\,dB$ given by $T_{tot} = \frac{\pi}{\sqrt{2}} \tau_0$ (2.63), ought to be much smaller than the extent of $e^{-(\frac{\beta_a t}{x_0 \gamma})^2}$ as well as much smaller than the variations of $m\left(\frac{\beta_a t}{\gamma}\right)$, these variations being the time resolution $\delta t$, which are derived from a rescalation of the spacial resolution $\delta x$, as seen in (3.15). This last condition is the most restrictive of the two.

Since the smallest variations will be of length $\delta x$, we have that in time the variations will be of the order:

$$\delta t = \frac{\gamma \delta x}{\beta_a} \qquad (3.15)$$

$$\delta t \simeq \frac{\gamma x_0 \pi}{N \beta_a \sqrt{2}} \qquad (3.16)$$

The time variation due to the mask has to be much longer than the time duration of the incoming pulse $(-10\,dB)$. This is:

$$\delta t \gg \Delta t_{10dB} \qquad (3.17)$$

$$\frac{\gamma x_0 \pi}{N \beta_a \sqrt{2}} \gg \frac{\pi}{\sqrt{2}} \tau_0 \qquad (3.18)$$

Simplifying:

$$\frac{\gamma x_0}{N \beta_a} \gg \tau_0 \qquad (3.19)$$

Which we will consider the condition for the spatial profile to be directly transformed into the time profile. We can understand this as if the time profile was a delta function when compared to the spatial one, and hence we obtain in time what we previously had in space but rescaled.

The maximum achievable frequency will be, by Nyquist criterion:

$$f_{max} = \frac{1}{2\delta t} = \frac{\beta_a}{2\gamma \delta x} \qquad (3.20)$$

The key advantage of using a SLM for spectral shaping is the real-time updatability of the SLM. This technique is specially useful for high-speed parallel-to-serial conversion (Daniel Leaird, 2000) where direct mapping from parallel (space) data to serial (time) data is often craved. The free-space optics based technique, however, has the difficulties of complicated alignment and high coupling loss (Nahar and Rojas, 2008).

## 3.1.2 Dispersive Fourier Transformation

Now it is presented a pulse shaping technique called Dispersive Fourier Transformation (DFT), also known as Frequency to Time Mapping (FTM). As mentioned before, this technique presents great analogy with DST. This procedure is based on dispersion, unlike DST, which was based on diffraction. Also, now it is the frequency spectrum, and not the spatial profile, which is translated into the time profile. As each frequency in a pulse travels at different velocity, each frequency has different time delays (2.37), provoking the ultrashort pulse to be temporally spread and when sufficiently dispersion is applied the time profile turns into a scaled replica of the frequency spectrum.

According to equation (2.43) and substituting in it equation (2.45) we obtain:

$$A(t,z) = \int_{-\infty}^{\infty} A(t',0) \frac{e^{\frac{j}{2\Theta}(t-t')^2}}{\sqrt{j2\pi\Theta}} dt' = \frac{e^{jt^2/2\Theta}}{\sqrt{j2\pi\Theta}} \int_{-\infty}^{\infty} A(t',0) e^{jt'^2/2\Theta} e^{-jtt'/\Theta} dt' \quad (3.21)$$

It shall be remembered that we are working in the frame of reference moving with the group velocity $v_g$.

If the pulse envelope is comprised in a sufficiently limited time width $\Delta t_0$ (FWHM) and the GDD is large enough, fulfilling the following condition (Solli, Chou and Bahram Jalali, 2007):

$$\left| \frac{\Delta t_0^2}{2\pi\Theta} \right| \ll 1. \quad (3.22)$$

Then the phase factor $\frac{-jt'^2}{2\Theta}$ becomes negligible as:

$$\left| \frac{jt'^2}{2\Theta} \right| \leq \left| \frac{\Delta t_0^2}{2\Theta} \right|. \quad (3.23)$$

And therefore expression (3.21) becomes:

$$\mathcal{E}(t,z) = \frac{e^{jt^2/2\Theta}}{\sqrt{j2\pi\Theta}} \int_{-\infty}^{\infty} A(t',0) e^{-jtt'/\Theta} dt'. \quad (3.24)$$

Expressing it as a function of the Fourier transform:

$$\mathcal{E}(t,z) = \frac{1}{\sqrt{j2\pi\Theta}} e^{jt^2/2\Theta} \mathcal{F}\{A(t,0)\}(w) \Big|_{w=\frac{t}{\Theta}} \quad (3.25)$$

This means that the output signal's envelope is the inverse Fourier transform of the incoming input one evaluated at frequency corresponding to $w = \frac{t}{\Theta}$, multiplied by a phase factor $\frac{t^2}{2\Theta}$ and a constant. When photo-detecting, because the electric signal is proportional to the square module of the signal (proportional to the electric power) this phase dependency, as well as the the term corresponding to the optical carrier disappear, and a temporal signal corresponding to the frequency spectrum is observed.

Thus, we are reproducing the frequency spectrum of the incoming pulse in the time domain, hence the name Frequency to Time Mapping.

In 2011, a less restrictive than (3.26) requirement was proposed (Torres-Company, D. E. Leaird and A. M. Weiner, 2011) based on the "antenna designer's formula", the criterion being:

$$\left| \frac{\Delta t_0^2}{\pi \Theta} \right| < 1 \tag{3.26}$$

This means introducing a phase error of $\frac{\pi}{8}$, equivalent to Fraunhoffer or far field approximation in space.

The applications of this technique are numerous. It can be used for real-time spectroscopy (Solli, Chou and Bahram Jalali, 2007). This is the most obvious one, since after dispersion and photodetection a rescaled version of the spectrum is obtained. In contrast to common electronic techniques, which require signal processing and are sometimes delimited by a narrow bandwidth, DFT spectroscopy offers real-time performance and is able through the wavelength-to-time rescalation operation to give place to waves belonging to the microwave frequency band, which can be captured by the photodetector (PD) and the real-time digitizer, to be analyzed in digital domain. The resolution will thus be determined by the bandwidth of the photodetector, the digitizer and also by the dispersion of the fiber (a bigger dispersion will increment the system's resolution).

Another application is Microwave Spectrum Sensing (C. Wang and Jianping Yao, 2012), frequently used in wireless-communications, radars, etc. Photonically assisted techniques have been proved to be superior to the electronic ones (C. Wang, 2014).

Modification of RF signals can also be achieved using DFT. One example is time reversal, later to be explained, signal compression and broadening are examples of this too. One of the applications of time reversal is found in wireless communications. Signal broadening is usually used for Analog to Digital Conversion (Solli, Chou and Bahram Jalali, 2007) as it increments the resolution of the ADC, enhancing the sampling rate by "slowing" down the analog MW signal. In contrast, signal compression (Jiejun Zhang and Jianping Yao, 2016) is often used for the purpose

of generating ultra-fast optic waveforms. Another application based on the same technique consists on performing the Fourier transformation of the input RF signal (H. Chi and J. Yao, 2007). All these time pulse shaping techniques are based in the same principle and set-up (Figure 3.2), with the only difference being the amount of dispersion of the second fiber (DF2 in Figure 3.2). In this thesis, time reversal will be the one to be deeply explained for its special utility in the field of wireless communications, very relevant nowadays.
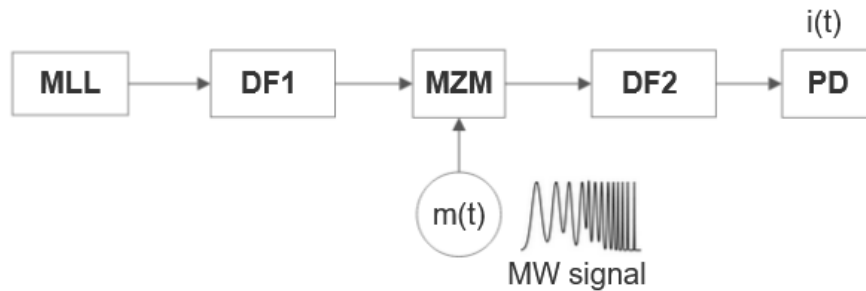


Figure 3.2: Set-up for temporal pulse shaping of Microwave signals. Composed of a Mode Locked Laser (MLL), a Dispersive Fiber (DF1), a March-Zender Modulator, another dispersive fiber (DF2) and a Photodetector (PD)

Arbitrary Waveform Generation (AWG) is one of its most important applications. The most common and simple technique for doing so consists on modulating the pulse spectrum coming out of the MLL. Then, the pulse goes through the dispersive fiber, becoming optically chirped and performing the wavelength-to-time mapping. At last, the optical pulse is photo-detected, in order to obtain the electrical signal, which is the envelope of the optical pulse. The set-up can be seen in Figure 3.3.
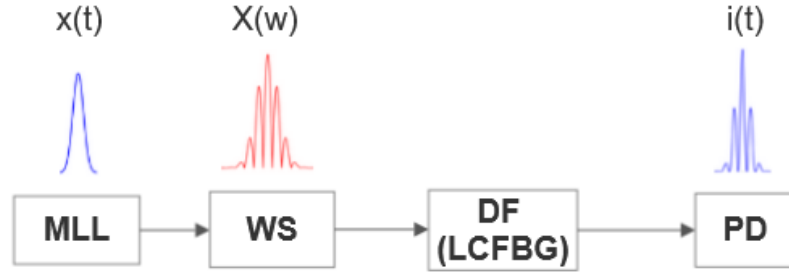
Figure 3.3: Set-up for AWG through DFT. Composed of a Mode Locked Laser (MLL), a Wave Shaper (WS), a Dispersive Fiber (DF) or alternately a Linearly Chirped Fiber Bragg Grating (LCFBG) and a Photodetector (PD)

The advantage of this method, in contrast with electronic ones (Lin, McKinney and A. Weiner, 2005), is the possibility of reaching ultrawideband signals, very demanded for radar and telecommunication applications.

### 3.1.2.1 The effect of propagation. TBWP of the AWG

As previously mentioned the non-chirped Gaussian pulse is transform limited. However, the introduction of a quadratic temporal phase, meaning a chirp of the pulse, broadens the time duration of the pulse. According to the expression (3.25), the signal obtained after the minimum required dispersion is proportional to the Fourier transform (frequency spectrum) of the pulse before dispersion, rescaled by a factor $|\Theta|$. The new time duration is then given by:

$$\Delta t = \Delta w |\Theta| \tag{3.27}$$

This happens without changing the modulus frequency spectrum profile, as the transfer function only introduces a phase variation. Hence, the bandwidth does not change. We can also see that this is the time duration looking at the broadening factor that we obtained for the initially non-chirped Gaussian pulse $M = \sqrt{1 + 4\Theta^2/\tau_0^4}$, when the condition (3.26) holds M can be approximated by:

$$M \simeq 2\frac{\Theta}{\tau_0^2} \tag{3.28}$$

Multiplying by the initial time duration:

$$\Delta t = 2\frac{\Theta}{\tau_0} \cdot \sqrt{2 \cdot ln2} \tag{3.29}$$

And substituting $\Delta w = \frac{2\sqrt{2ln2}}{\tau_0}$ (2.61) in equation (3.27) yields the same result for the FWHM time duration.

To generate an arbitrary waveform, the pulse has to be spectrally shaped. Thus, the TBWP of the generated microwave signal is limited, as it will be derived, by the spectral resolution of the pulse shaper. Since the signal will not any longer have a Gaussian profile (in time nor in spectrum), it is hard to say, a priori, what the duration and bandwidth of the pulse are. We will continue taking $\Delta w$ as the FWHM. The set-up employed for AWG is shown in figure 3.3. We will assume that the ML laser covers the full bandwidth of the spectral shaper (B). Thus, the bandwidth of the optical pulse after the shaper comes given by $\Delta w_{opt} = k_1 B = k_1 N \delta w$, where N is the number of spectrally resolved pulse shaper control elements ("resolution elements" in the following) and $\delta w$ is the spectral resolution. The constant $k_1$ is because, $\Delta w_{opt}$ is the FWHM and B is just the total bandwidth of the spectrum, $k_1$ is the factor that relates them and it will come given by the pulse's shape after the WS. As seen in (3.27), the pulse time duration widened after dispersion is the bandwidth multiplied by the GVD:

$$\Delta t = k_1 N \delta w |\Theta| \tag{3.30}$$

Now, to calculate the electrical bandwidth we take into account that the maximum achievable frequency $f_{max}$ in Hz is (Rashidinejad and A. M. Weiner, 2014):

$$f_{max} = \frac{1}{2\delta t} \tag{3.31}$$

Where $\delta t = \delta w \Theta$ is the highest time resolution achievable.

$$f_{max} = \frac{1}{2\delta w |\Theta|} \tag{3.32}$$

Or in rad/s:

$$w_{max} = \frac{\pi}{\delta w |\Theta|} \tag{3.33}$$

With a factor 2 dividing due to the need of at least two resolution elements in order to create one sinusoidal cycle (one for the positive half-cycle and one for the negative half-cycle).

As done previously, in order to keep the derivation general, we introduce a constant $k_2$, which will depend on the specific pulse shape, therefore:

$$\Delta w_{RF} = k_2 w_{max} = k_2 \frac{\pi}{\delta w |\Theta|} \tag{3.34}$$

Finally, the TBWP is:

$$TBWP = k_1 k_2 N\pi = KN\pi \tag{3.35}$$

Where $K = k_1 k_2$ and it depends on the shape of the generated waveform.

As an example to give values to this $K$, we will analyze the case of a an electrically chirped waveform with a Gaussian envelope. These MW are specially interesting because of their high bandwidth. We will suppose here that the bandwidth of the pulse shaper covers almost the whole laser spectrum. According to expression (2.61) and (3.27) the maximum possible time duration of the signal, with the FWHM criterion, is :

$$\Delta t \simeq \Delta w_{ini} |\Theta| = \frac{2\sqrt{2ln2}}{\tau_0} |\Theta| \tag{3.36}$$

The bandwidth of the chirped signal is estimated as half of the chirp tuning range, with its value being half of the maximum instantaneous frequency achieved $f_{max}$. Hence the $BW$ of the RF signal is approximately, (Mei, Y. Xu et al., 2015):

$$\Delta w_{RF} \simeq \frac{1}{2} w_{max} = \frac{\pi}{2\delta w |\Theta|} \tag{3.37}$$

Hence, multiplying the latter with the time duration, we obtain:

$$TBWP \simeq \frac{\pi\sqrt{2ln2}}{\tau_0 \delta w} \qquad (3.38)$$

From the latter, it may seen that the TBWP depends on the initial pulse. However, the spectral resolution and the initial time duration are directly related. Since the spectral filter covers almost the whole pulse bandwidth, then B can be taken as $B \simeq 2\pi/\tau_0$, covering most of the pulse intensity (B is the full width at $-10dB$ maximum) and also remembering that $B = N\delta w$. Then (3.38) is simplified to:

$$TBWP \simeq \frac{N\sqrt{2ln2}}{2} \qquad (3.39)$$

Hence, K in equation (3.35) is for this case:

$$K \simeq 0.187 \qquad (3.40)$$

The main conclusion given by these expressions is that the TBWP does only depend on the number of resolution elements and the shape of the outgoing pulse (when calculating it for the FWHM), showing that increasing the resolution elements of the spectral shaper allows to augment the TBWP of the generated MW signal. Increasing the dispersion allows longer duration of the RF wave, but it also reduces the maximum achievable frequency and hence the bandwidth of the signal.

Although the achievable bandwidth is really high and not allowed by electronic techniques, Weiner et al. proposed an improved set-up that could achieve twice the bandwidth of the one we have presented (Rashidinejad and A. M. Weiner, 2014). This can be explained because the generated waveforms with the set-up shown in figure 3.3 are baseband, and therefore the maximum bandwidth is achieved only by amplitude spectral shaping, and therefore to generate the fastest sinusoidal cycle at least two resolution elements are needed, while the one presented by Weiner et al. has a programmable passband component that doubles the achievable TBWP (Rashidinejad and A. M. Weiner, 2014), reaching the upper bound limit given by $f_{max} = \frac{1}{\delta w |\Theta|}$ and its corresponding bandwidth.

## 3.2 Time-reversal

The development of these generation techniques for ultrawideband microwave signals has induced to develop systems for their transmission and detection (R. Qiu, J.Q. Zhang and Guo, 2006), specially in rich multipath wireless communications, that reduce the cost and energy of the whole communicating system. Time reversal (TR) has been presented as a new paradigm, offering good data transmission rate, stability (R. C. Qiu et al., 2006) and simplicity. Systems employing this technique are based on precoding the transmitted symbols from one or several antennas with the time reversed version of their respective channel impulse response, allowing to focus the signal in space, power and time at the receiver (Oestges, 2004).

Several ways to reverse a signal are employed nowadays, being digital processing among the most used. Nevertheless, photonic time reversal of radiofrequency waves has been recently developed, offering the advantages of good real-time performance, high time-bandwidth product and high accuracy (Z. Wang et al., 2019), which is of high interest when treating with ultra-wide bandwidth signals.

Here, we shall propose a scheme for TR by photonic means. For this end we will make use of the previously explained DFT technique.

The scheme, shown in Figure 3.4, consists on a mode-locked laser (MLL) to generate an ultrashort Gaussian pulse, a linear dispersive element with GVD $\Theta_1$ , a March-Zender modulator, another dispersive element with GVD $\Theta_2 = -2\Theta_1$, which can be achieved with two dispersive elements with a GVD equal to $-\Theta_1$, and a photodetector. An optical filter with a bandwidth centered at the MLL carrier frequency can also be added after the MLL, in order to achieve a flatter spectrum.

The set-up is the one presented in Figure 3.4. The second dispersve fiber can consist in one with the double and opposite dispersion of the first or 2 dispersion fibers with opposite sign to the first one, which may be easier to obtain.
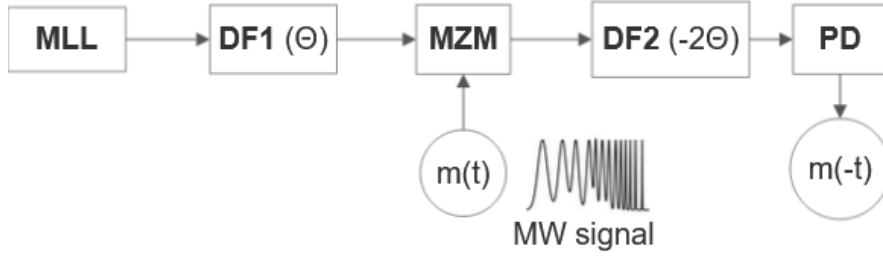
Figure 3.4: Set-up for Time Reversal through DFT. Composed of a Mode Locked Laser (MLL), a Dispersive Fiber (DF), a March-Zender Modulator, another dispersive fiber (with a dispersion value twice the first one and opposite sign) and a Photodetector (PD). What we will obtain in the output is not exactly the reversed signal, but the electrical current proportional to the reversed signal.

Mathematically, this writes as follows (Jiejun Zhang and Jianping Yao, 2015). The pulse coming from the MLL, with bandwidth $BW_{opt}$, goes through the first dispersive element:

$$g(t) \propto p(t) * e^{\frac{jt^2}{2\Theta_1}}, \tag{3.41}$$

where the constant of the transfer function has been omitted for simplification and $p(t)$ is the Gaussian pulse coming out the MLL (or of the optical filter if we put one). The broadened pulse is then multiplied in the MZM by the microwave signal $m(t)$ we want to reverse.

$$s(t) = g(t) \times m(t). \tag{3.42}$$

Afterwards, the signal goes through another dispersive element, with a dispersion coefficient opposite to the first fiber.

$$b(t) \propto s(t) * e^{\frac{jt^2}{-2\Theta_1}}. \tag{3.43}$$

Omitting once again the proportionality constant. Substituting (3.41) and (3.42) in (3.43):

$$b(t) \propto p(t) * e^{\frac{jt^2}{2\Theta_1}} \times m(t) * e^{\frac{jt^2}{-2\Theta_1}}, \tag{3.44}$$

$$b(t) \propto p(t) * M(w)|_{w=\frac{-t}{\Theta_1}}, \tag{3.45}$$

where to go from the first to the second equation we have used the results obtained in the DFT section 3.1.2.1, with $M(w)$ being the Fourier transform of the microwave signal $m(t)$, $M(w) = \mathscr{F}\{m(t)\}(w)$.

Then the signal goes through the last fiber, with $GVD = -\Theta_1$:

$$f(t) \propto b(t) * e^{\frac{jt^2}{-2\Theta_1}}, \tag{3.46}$$

Expressing it as a function of the frequency spectrum, by (3.25):

$$f(t) \propto e^{\frac{jt^2}{-2\Theta_1}} B(w)|_{w=\frac{-t}{\Theta_1}}, \tag{3.47}$$

using the result in (3.45):

$$f(t) \propto e^{\frac{jt^2}{-2\Theta_1}} \left[\mathscr{F}\{p(t) * M(w)|_{w=\frac{-t}{\Theta_1}}\}(w)\right]_{w=\frac{-t}{\Theta_1}}, \tag{3.48}$$

the above may be rewritten as:

$$f(t) \propto -e^{\frac{jt^2}{-2\Theta_1}} \Theta_1 \left[P(w) \times m(\Theta_1 w)\right]_{w=\frac{-t}{\Theta_1}} \tag{3.49}$$

and finally we arrive to:

$$f(t) \propto -e^{\frac{jt^2}{-2\Theta_1}} \Theta_1 P(w)|_{w=\frac{-t}{\Theta_1}} \times m(-t). \tag{3.50}$$

In the detector the phase-term is removed as $i(t) = \mathscr{R}|f(t)|^2$, where $\mathscr{R}$ is the responsivity of the photodiode, and hence the expression for the electrical current is:

$$i(t) \propto |P(w)|_{w=\frac{-t}{\Theta_1}}|^2 \times |m(-t)|^2 \tag{3.51}$$

The obtained waveform is the reversed electrical signal multiplied by constants and by $|P(w)|_{w=\frac{-t}{\Theta_1}}|^2$. For a given time duration, later to be specified, and a time short enough pulse, the latter can be considered to be constant, since the spectrum of a sufficiently short $p(t)$ can be considered ideally to be flat. Therefore, obtaining a waveform directly related to the reversed RF signal.

The maximum time duration of the microwave signal to be reversed is given by the

range in which this $P(w)|_{w=\frac{-t}{\Theta_1}}$ is non-zero and approximately with the same value all over time. If we suppose we put (after the MLL) a band-pass filter with an approximately flat response with a bandwidth $BW_{OF}$, the time duration of the pulse $p(t)$ after being stretched, according to (3.27), is :

$$\tau = BW_{OF} \times |\Theta_1| \qquad (3.52)$$

Hence, this will also be the maximum duration for the RF signal. If there is not such filter, the $\tau$ at FWHM will be $\tau = BW_{opt} \times |\Theta_1|$.

## 3.2.1 Bandwidth limitation

In the latter we have seen that the total time duration of the MW signal to be reversed is $\tau = BW_{opt} \cdot |\Theta_1|$. When not applying an optical filter, and the pulse is stretched directly after the MLL, therefore with a Gaussian envelope, we can define the time duration for the FWHM as we did in (3.36), often named as $\tau_{3dB}$ (Z. Wang et al., 2019) since the FWHM corresponds to a 3dB lost in power. It comes given by:

$$\tau_{3dB} = \frac{2\sqrt{2ln2}}{\tau_0}\Theta_1 \qquad (3.53)$$

The bandwidth is also limited. Among the possible bandwidth limitations, those concerning the electronic devices, such as the PD or the MZM can nowadays be neglected, since they can reach up to 100 GHz (Jiejun Zhang and Jianping Yao, 2015). The other components that might cause a limitation in the bandwidth are the optical ones, the initial pulse bandwidth is limited at FWHM by (2.61), so the Gaussian limited pulse coming out of the laser has a $\Delta w_{3dB} = \frac{2\sqrt{2ln2}}{\tau_0}$, but this is too large to cause any bandwidth limitations compared with other factors.

There is also a dispersion penalty for the case of optical intensity modulation that results from the "interference between the carrier upper sideband and carrier lower sideband beat terms" (Yan Han and Bahram Jalali, 2003), or also known as double side band penalty. This bandwidth limitation for the case of time reversal expressed

in Hz as the FWHM ($\Delta f_{3dB}$) is (Mei, B. Xu et al., 2016) (Y. Han and B. Jalali, 2003):

$$\Delta f_{3dB} = \sqrt{\frac{1}{4\pi|\Theta|}} \qquad (3.54)$$

Another possible cause for bandwidth limitation can be the dispersive element's nature. If instead of dispersion compensation fibers we used linearly chirped fiber Bragg gratings, the bandwidth will come given by the bandwidth of the LCFBG, which don't allow transmission of the whole frequency spectrum.

# Chapter 4

# Results and simulations

## 4.1 Direct Fourier Transformation

Also known as Frequency to Time mapping, this technique was presented in section 3.1.2.1. Now, we shall give numbers and present the results obtained that prove the validity of the theory. As usual, the input pulse will consist on a Gaussian pulse, coming out of a mode-locked laser. Usually the MLL does not give pulse with an exact Gaussian envelope. However, using an optical filter we could reach the desired shape. The Gaussian pulse we propose for this simulation has $\tau_0 = 60$fs, according to expression (2.58), and hence a time-duration (FWHM (2.60)) of 70.71fs. The pulse at $z = 0$ can be seen in Figure 4.1.
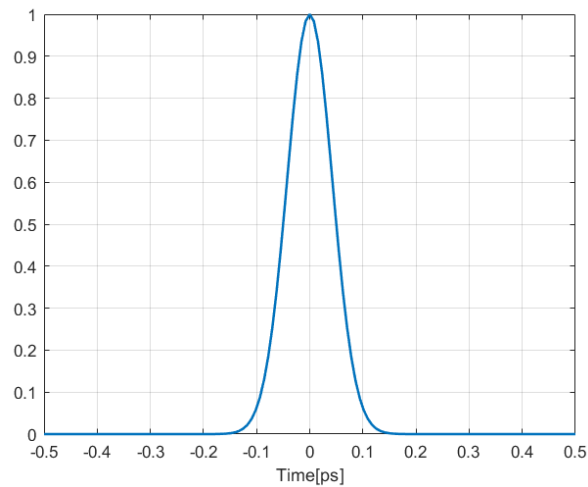


Figure 4.1: Incoming pulse envelope, $p(t)$.

The pulse goes then through a wave-shaper. This wave-shaper just models the amplitude of each frequency contained in the wave spectrum. In our case we will assume that the shaper multiplies the incoming signal in the frequency domain by a cosinus function of period $T_1 = 1.2566$ THz. The spectral mask is shown in Figure 4.3. Hence, the obtained signal in Figure 4.4 comes given by the Fourier transform of the incoming signal 4.2 multiplied by the spectral mask, giving place to Figure 4.4. Thus, the modulus of the spectrum, will show a periodicity of half of that of the signal $T_2 \simeq 0.6283$ THz.

Mathematically the pulse after going through the wave shaper is expressed in the frequency domain as:

$$G(w) = P(w) \cdot M(w), \tag{4.1}$$

where $P(w)$ is the Fourier transform of the input Gaussian pulse and $M(w)$ is the spectral mask function.
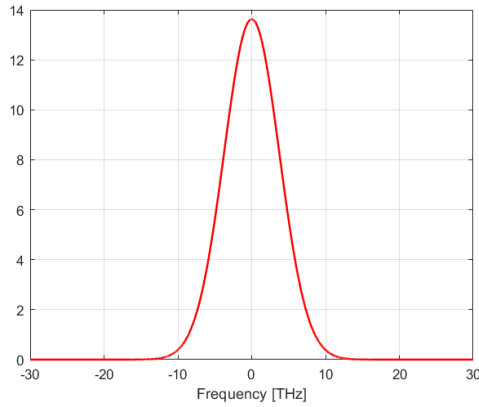


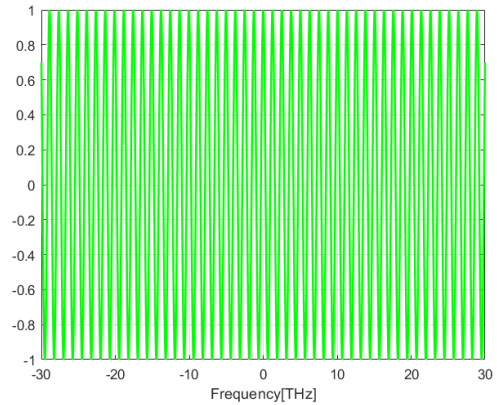Figure 4.2: Outcoming signal in the frequency domain, $P(f)$.



Figure 4.3: Mask $M(f)$.

Since we will photodetect the square of the absolute value of the incoming field temporal envelope, the obtained signal in the temporal profile will be a scaled replica of the modulus of the spectrum power to the square and multiplied by some constant, as seen mathematically from expression 3.25. Hence, it is the modulus of the signal whose period we are interested in.
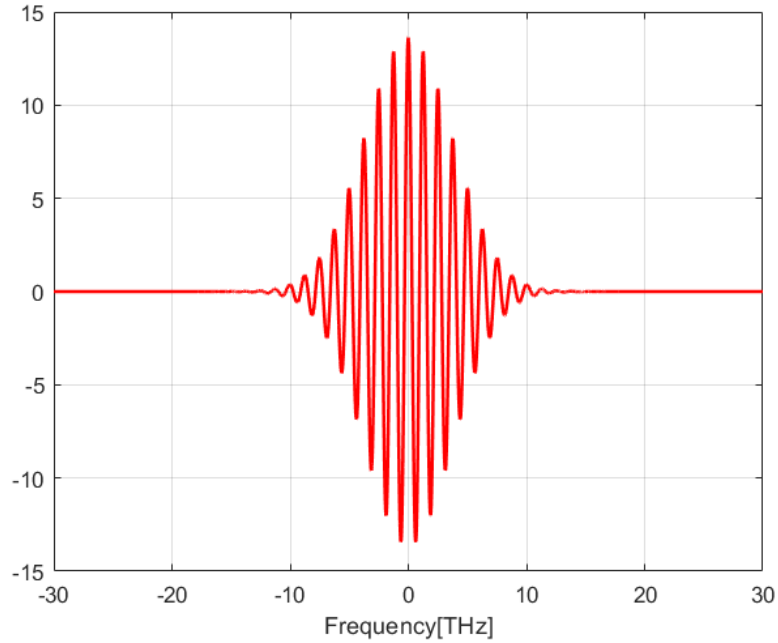
Figure 4.4: Outcoming signal in the frequency domain, $G(f)$

The waveshaper only modifies the amplitude of each frequency component, not its phase. Thus, the phase of each frequency will come given by the pulse coming out of the MLL. With the phase, theoretically, being equal to zero. This is shown in Figure 4.5.

The oscillations in the borders are because when the amplitude is 0 the phase is not well defined.

After the shaping of the pulse, it goes through the dispersive fiber. We propose a dispersive coefficient at $\lambda_0$=1550 $nm$ of $17\frac{ps}{nm \cdot km}$, the typical D in standard single-mode fibers, and a length of 100 $m$. A GDD of $-2.167\ \frac{ps^2}{rads}$ is obtained. As the transfer function of the dispersive fiber is $H(w) = e^{-j\Theta w^2/2}$, it induces a quadratic phase in the incoming pulse (Figure 4.6), provoking different time delays in different frequencies, and hence inducing a chirp as it is seen in Figure 4.7.

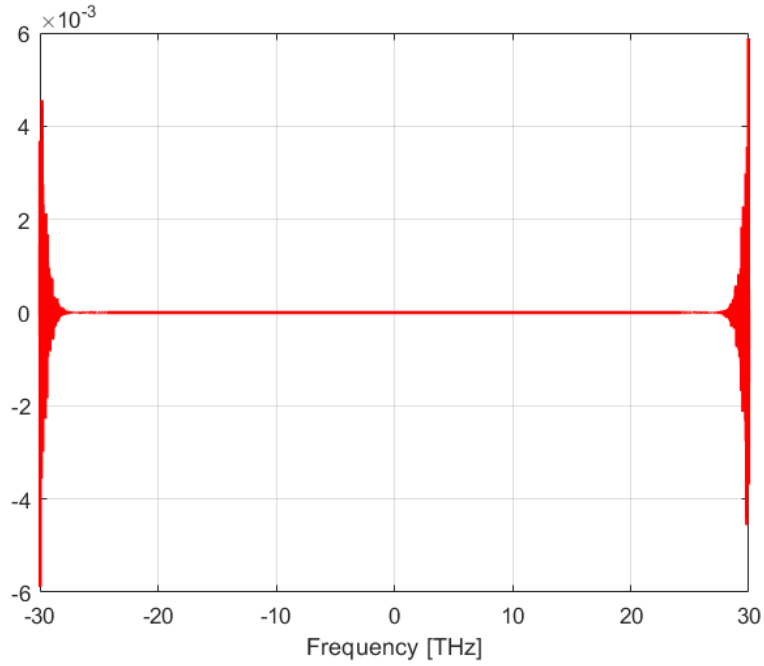In the frequency domain this reads:

$$S(w) = G(w) \cdot H(w). \tag{4.2}$$
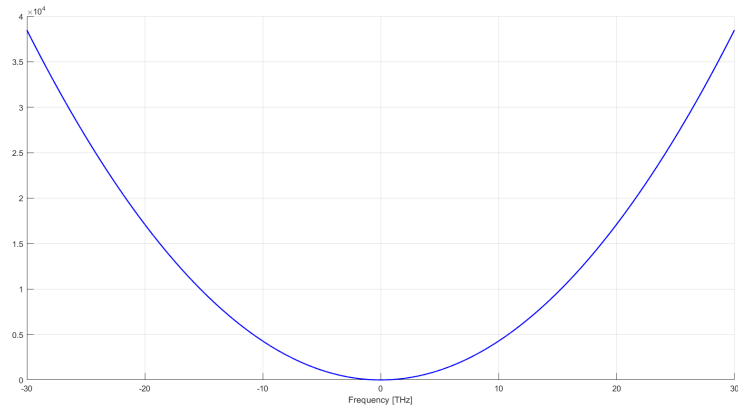
Figure 4.5: Phase of the input signal, G(f)



Figure 4.6: Phase after dispersion, S(f)

Using the expression derived in (3.25) for the conditions required for dispersion and incoming pulse duration, which are met here for the chosen values, we can express the field envelope in the time domain as:

$$s(t) = Ke^{-jt^2/2\cdot 2.167\frac{ps^2}{rads}}G(w)\Bigg|_{w=\frac{t}{-2.167\frac{ps^2}{rads}}} \tag{4.3}$$

where $K$ is the constant derived in (3.25), but we are only interested in the proportional temporal varying terms.
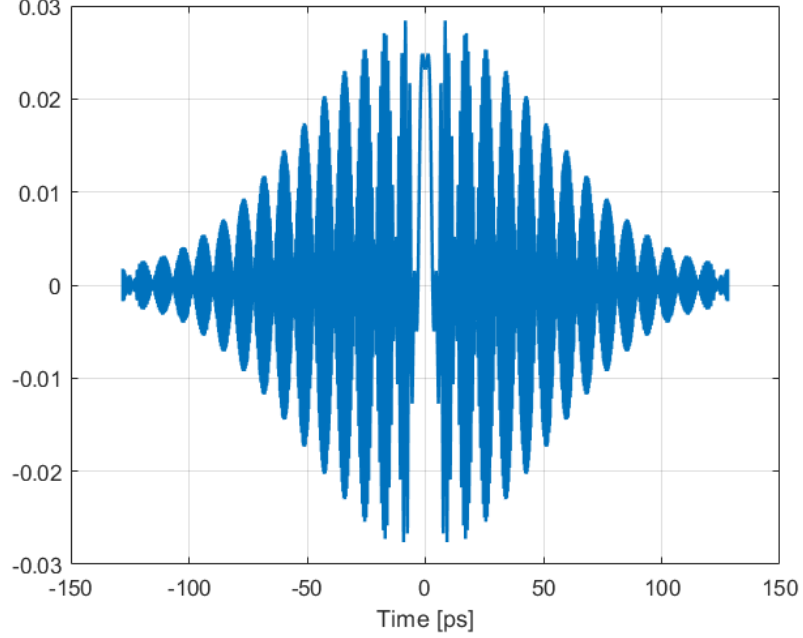


Figure 4.7: Output chirped signal, s(t)

Nevertheless, it must be reminded that the phase is periodic in $2\pi$. According to (3.27) the time duration will be $T_{dur} = \Delta w \cdot GDD$. We take $\Delta w$ as the FWHM (2.61), $\Delta w = 39.21 \cdot 10^{12}$rads/s (6.24 THz). The time duration being then:

$$T_{dur(FWHM)} = 39.21 \cdot |-2.167| = 84.96ps \qquad (4.4)$$

The definition we have taken also for time is the FWHM of the Gaussian envelope. To calculate the approximate time duration at $-10\ dB$, we can take the $\Delta w_{tot} = 2\pi/\tau_0 = 104.62 \cdot 10^{12}$ rads/s, covering most of the pulse intensity, as we did for the TBWP example.

$$T_{tot} = 226.69ps \qquad (4.5)$$

Figure 4.8 proves the validity of the approximations. After photodetection, the square of the absolute values of the signal are obtained $i_{pd}(t) = |s(t)|^2$. The final signal is:
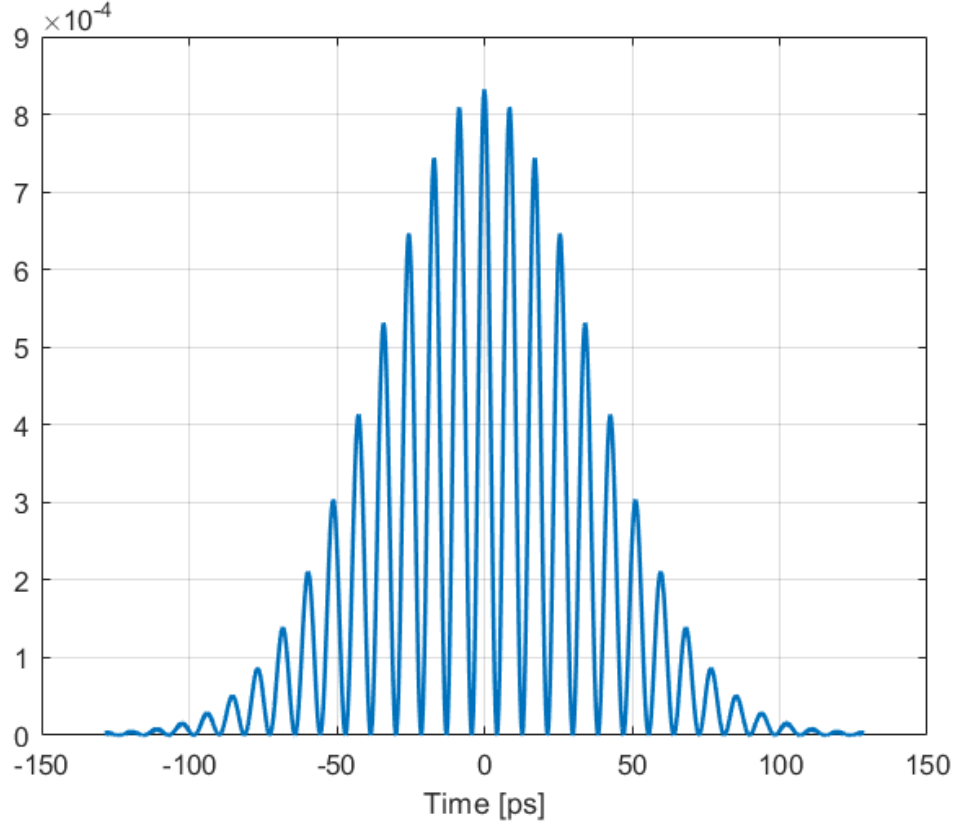
Figure 4.8: Final output RF signal

Mathematically it writes:

$$i_{pd}(t) = K^2 \left| G(w) \right|_{w=\frac{t}{-2.167\frac{ps^2}{rads}}}^{2} \tag{4.6}$$

The frequency of this RF signal can also be calculated. The period of the microwave signal will be:

$$T_{RF} \simeq T_2 \cdot |\Theta| = 0.6283\,THz \cdot 2\pi\,\frac{rad}{s} \cdot |-2.167|\,\frac{ps^2}{rad} \simeq 8.554\,ps \tag{4.7}$$

As the period of the modulus of the frequency spectrum $T_2$ is broadened by $|\Theta|$ after dispersion.

The microwave frequency will then be:

$$f_{RF} = \frac{1\pi}{T_{RF}} \simeq 116.9\,GHz \tag{4.8}$$

## 4.1.1 TBWP

Now we will calculate TBWP for a generated chirped microwave with a Gaussian envelope, according to the definitions of $T_{FWHM}$ and bandwidth being equal to $\frac{f_{max}}{2}$. We will take the same value we have used for the previous section of $\tau_0$ for the input Gaussian pulse, as well as the same dispersion value. As stated by (3.40), the total product should be $TBWP \simeq 0.187N\pi$, where N is the number of resolution elements of the spectral shaper. We suppose that the spectral shaper range is equal to the full width of the laser pulse at $-10\ dB$. Thus, the bandwidth of the pulse and of the spectral shaper is $BW_{tot} \simeq 16.6524$ THz (from the previous section 3.1.2.1 $\Delta w_{tot} = 2\pi/\tau_0 = 104.62 \cdot 10^{12}$ rads/s). The resolution $\delta f$ is equal to half the smallest period (in the frequency domain) of the modulus of the mask's linearly chirped cosinus. This will be $\delta f = \frac{0.6283}{2}\ THz = 0.3141$ THz, the same as the one used previously. Then the total number N of resolution elements is:

$$N = \frac{BW_{tot}}{\delta f} = \frac{16.6524}{0.3141} \simeq 53 \tag{4.9}$$

And the TBWP:

$$TBWP \simeq 0.187N\pi \simeq 31.14 \tag{4.10}$$

This is the result given by theory. Checking out the result given by simulations (considering the BW as $\frac{f_{RF}}{2}$). Taking into account that the dispersion, the initial Gaussian pulse and the spectral resolution are the same as in the previous simulation, the $T_{dur}$ and the $f_{max}$ will also be the same:

$$TBWP = T_{dur} \cdot \frac{f_{RF}}{2} \cdot 2\pi = 84.96 \cdot \pi \cdot 0.1169 = 31.2 \tag{4.11}$$

It can be seen that these two results are almost exact, proving the validity of the derived theory and showing that an increment of the resolution of the waveshaper will also mean an increment of the achievable TBWP. These result can also be visualized in Figures 4.9 and 4.10.
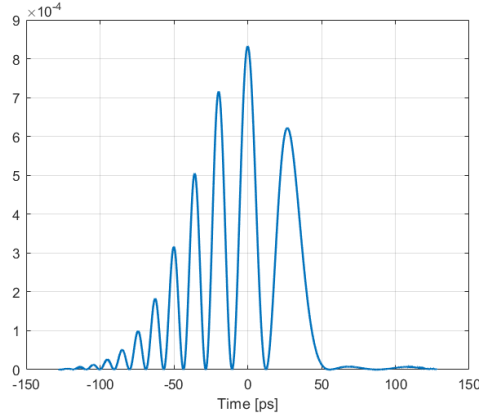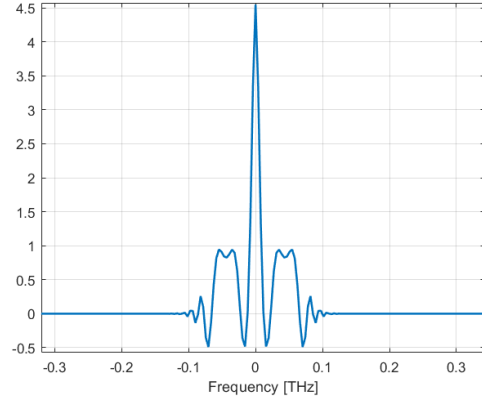
Figure 4.9: Output signal in the time domain.



Figure 4.10: Output signal in the frequency domain.

## 4.2 Time reversal

One application that has been discussed in the techniques section is the time reversal of a microwave signal through photonic means. In order to do so, high dispersion is needed, as it will be now seen, for signals up to a few nanoseconds. One problem found in simulations is that for long periods of time (up to 10 ns) the combination of long times and high enough spectral resolution is challenging and outranges the available computer power. This has prevented us from being able to simulate an approximately plane optical filter for the incoming pulse. However, the existence of an analytical expression of the dispersion of a Gaussian pulse (2.53), has allowed us to perform a proper and interesting simulation, with good results.

The simulation will consist then, as proposed in 3.2, in a Gaussian ultrashort pulse going out of a MLL, then through dispersion, multiplied by a microwave signal, dispersed again (with dispersion coefficient equal to two times the first one but opposite sign) and finally photodetected by a PD (the OF has been removed from simulation). The set-up is shown in Figure 3.4. We know from (3.27) that the time duration of the pulse after going through dispersion is $T = \Delta w |\Theta|$ .The signal that we want to time-reverse and multiply by the pulse with the MZM has a duration of approximately 10 ns. We suppose a total dispersion of $D = 1450 \frac{ps}{nm}$ ($\Theta = -1848 \frac{ps^2}{rads}$ for $\lambda_0 = 1550\ nm$). Hence, the approximately flat bandwidth of the incoming pulse

has to be of 0.861 THz or bigger. The longest the FWHM bandwidth of the pulse the better, since we want the spectrum to be as flat as possible and that will happen if the Gaussian pulse is wide enough so that the center of the spectrum can be considered constant. The Gaussian pulse made by the MLL will have a $\tau_0 = 110fs$ (2.58) (Figure 4.11), right within the reach of state of the art MLL.
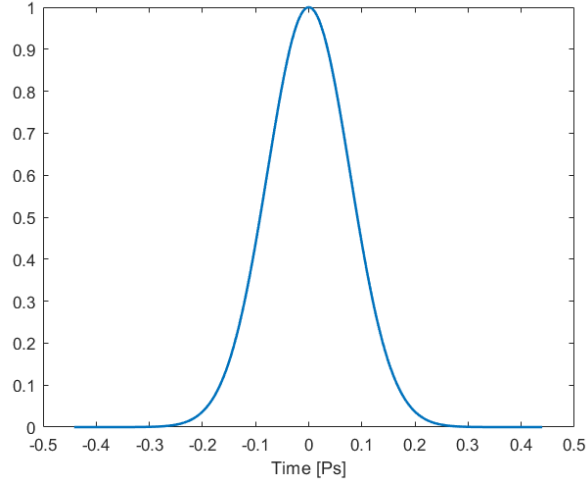


Figure 4.11: Time profile of the incoming Gaussian pulse, $p(t)$.

This means a $BW = 3.407$ THz (FWHM). We can consider the 0.861 THz in the center of the spectrum $P(w)$ as flat (this value is the Full Width at $0.9567$ maximum, corresponding to $-0.45dB$) (Figure 4.12), we will see later in results that this is good enough. Taking less dispersion or a longer time pulse would make $P(w)|_{w=\frac{-t}{\Theta}}$ in expression (3.51) less constant for this interval, causing some decay in the borders of the reversed microwave signal. If the time of the signal were reduced, this distortion would once again disappear.
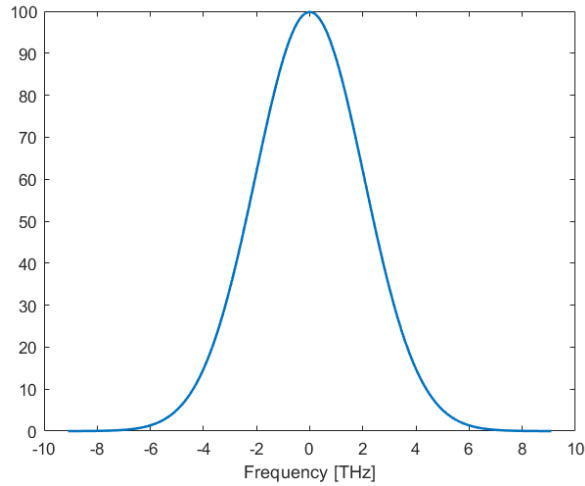
Figure 4.12: Frequency profile of the input Gaussian pulse, $P(w)$

The pulse $p(t)$ then disperses through the medium, performing a DFT leading to an extended Gaussian pulse. The expression after this step is $G(w)=P(w)H_1(w)$, where $P(w)$ is the Fourier transform of the Gaussian pulse and $H_1(w)$ the transfer function of the dispersive fiber. In figure 4.13, it is shown the absolute value of the time profile of the broadened pulse, after dispersion the pulse $g(t)$ conserves the Gaussian envelope, but broadened, being it almost flat (very low variation) over a time of more than 10 ns and becoming optically chirped.
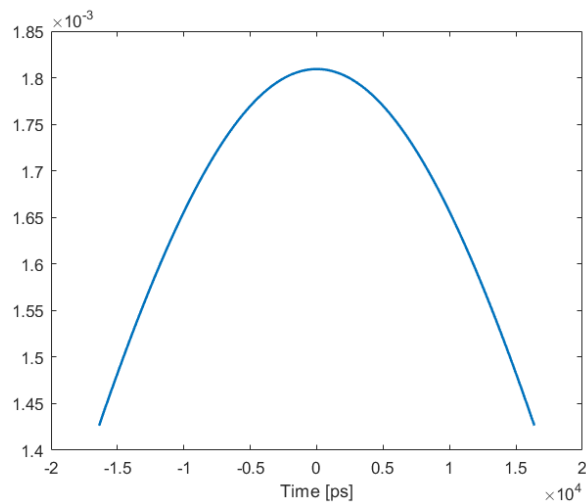


Figure 4.13: Time profile of the pulse after going through dispersion (absolute value), $|g(t)|$.

This signal is multiplied by the RF signal $m(t)$ shown in figure 4.14. This is done in the MZM.
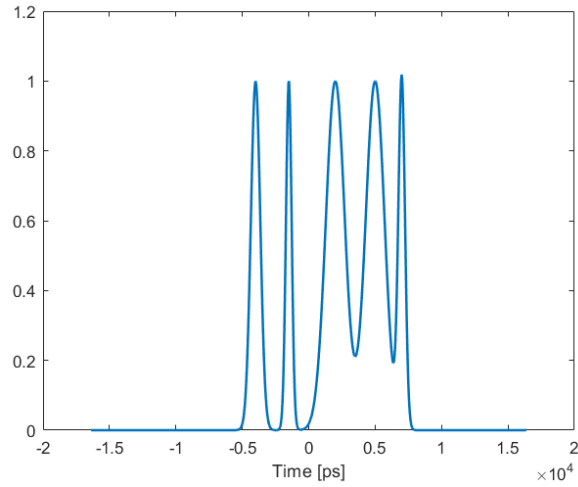


Figure 4.14: Time profile of the RF signal, $m(t)$.

This will lead to a chirped signal with the RF signal's envelope $(s(t)=g(t) \cdot m(t))$. As it is seen in figure 4.15.
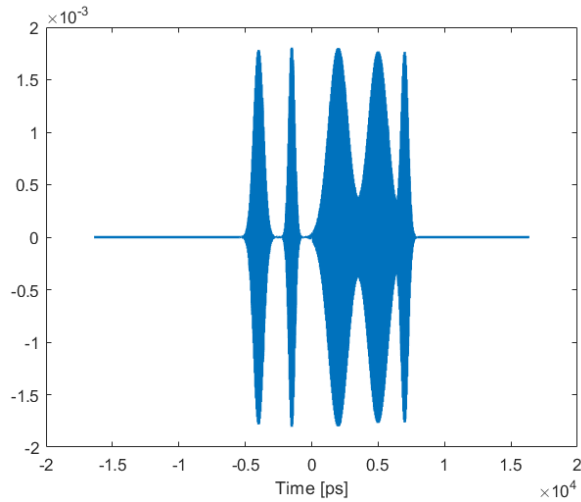


Figure 4.15: Time profile of the chirped RF signal, $s(t)$.

Dispersion is applied once again $(F(w)=S(w) \cdot H_2(w))$. This time with a value twice the first and with opposite sign. Meaning a total dispersion of $D_2 = -2900 \frac{ps}{nm}$. The signal at the end of the fiber will then be proportional to the microwave signal,

but reversed (as explained in section 3.2). One thing that might have to be done in the laboratory is amplify the signal, as its amplitude after dispersion can become too low to be photodetected. The reversed signal in the time domain can be seen in Figure 4.16.



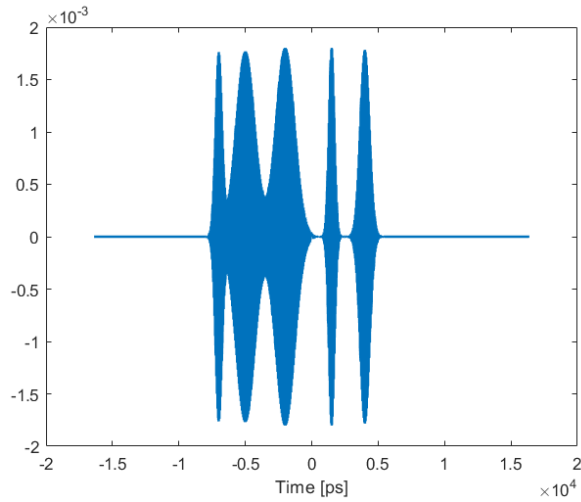Figure 4.16: Time profile of the chirped RF signal after going through the second dispersive element, $f(t)$.

Then the signal is photodetected, since the electrical intensity is related to the optical power, we obtain an intensity proprtional to the square of the signal's envelope (Figure 4.17), $i_{pd}(t) \propto |f(t)|^2$.
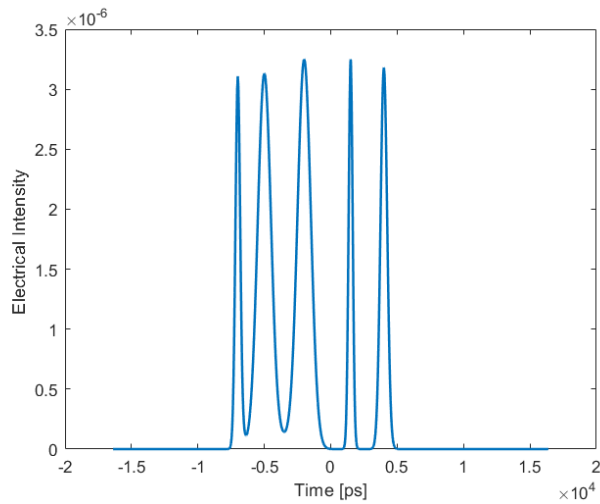


Figure 4.17: Intensity of the electric signal obtained after photodetection

To see the accuracy of this technique and the numbers used in this section we will compare the intensity of the original MW signal and the reversed one flipped. Both signals are re-normalized, as the intensity is reduced when multiplying by the broadened photonic signal and hence the reversed one will be less intense, but this can be easily corrected by using an amplifier.
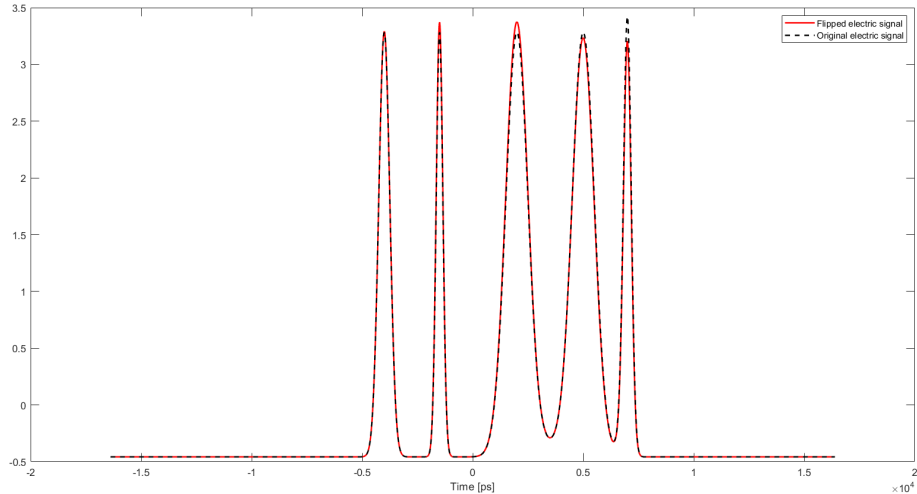


Figure 4.18: Comparison of renormalized intensities (the reversed one being flipped)

From the figure 4.18, it becomes clear that the dispersion is high enough and the values taken are sufficiently good, so that the two signals almost overlap. This is confirmed by the correlation, with an R-squared $(R^2)$ equal to $R^2 = 0.9991768$, almost 1, which can be considered a nearly perfect correlation.

## 4.2.1 Bandwidth limitation

In the previous simulation, no bandwidth limitation has been observed, since these signals do not exceed the highest bandwidth limitation frequencies. As mentioned in subsection 3.2.1, this limitation may be caused by double sideband effects. Now, we show how the bandwidth limitation distorts the reversed signal causing an imperfect time-reversal. We consider a chirped signal going from lower to higher frequencies,

formed by Gaussian pulses of different time duration (highest to lowest). This microwave signal to be reversed is shown in Figure 4.20.
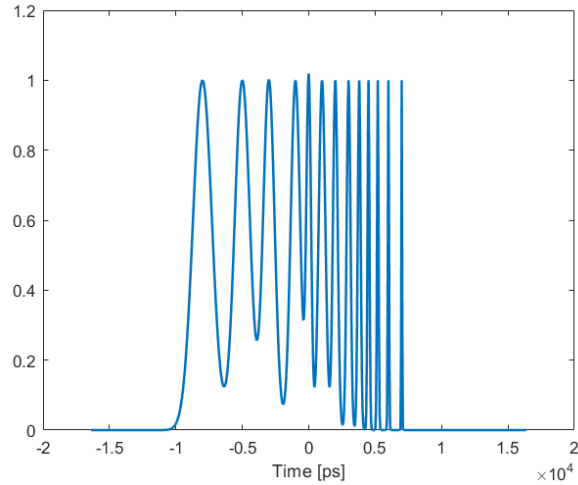


Figure 4.19: Input MW signal

From equation (3.54) we know that the maximum bandwidth allowed without losing more than half the intensity goes up to $\sqrt{\frac{1}{4\pi|\Theta|}}$ being $\Theta$ the dispersion of the first fiber. The total Gaussian pulse envelope bandwith (fullwidth at $-10\,dB$) is approximately $BW = \frac{1}{\tau_i}$ in Hz (seen in 2.2). Hence when the latter is bigger than (3.54) the pulse will suffer a dispersion power penalty causing the signal to be badly reversed. This will happen when:

$$\frac{1}{\tau_i} > \sqrt{\frac{1}{4\pi|\Theta|}} \tag{4.12}$$

$$\tau_i < \sqrt{4\pi \cdot \Theta} \tag{4.13}$$

For the previous value of total dispersion $D = 1450\,\frac{ps}{nm}$ ($\Theta = -1.8481\,ps^2$) the limit will be:

$$\tau_{lim} \simeq 139ps \tag{4.14}$$

Hence, the Gaussian pulses with $\tau_i < \tau_{lim}$ will be distorted by dispersion. In figure 4.20 this is the case for the 4 last pulses with the narrowest width (100 ps, 80 ps, 60 ps and 40 ps respectively). When applied to the time-reversal set-up we obtain Figure 4.20.
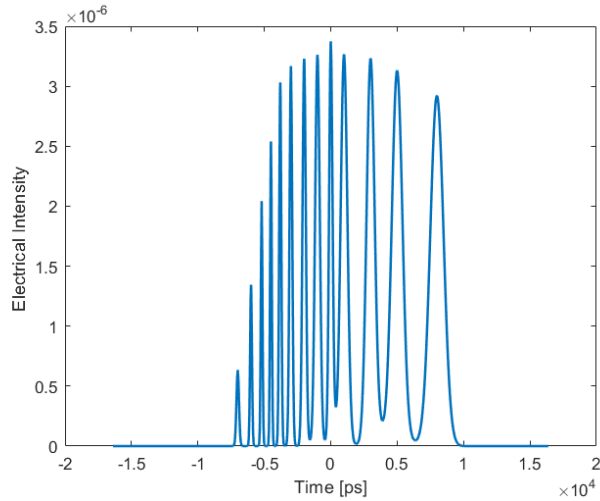
Figure 4.20: Output electric signal

We observe that the last pulse to not be very distorted is the fifth in the reversed signal $\tau_i = 150ps$ and the first 4 are more affected, it is also seen that the higher the bandwidth the most distorted the pulse becomes. This is only because of the power penalty and not because the extended pulse is not flat or long enough (it has been checked that higher dispersion values only cause higher distortion). If we compare once again the flipped signal and normalize both of them, we obtain figure 4.21. Clearly showing the distortion of the narrowest pulses, confirmed by an $R^2$ of 0.9813, still quite good but much lower than the one obtained before for lower bandwidth pulses.



Figure 4.21: Output electric signal

# Chapter 5

# Conclusions

In this work, we have provided an in-depth analysis of photonic arbitrary waveform generation (AWG) techniques based on space and frequency to time mapping, with eyes to unveiling their potential for microwave applications.

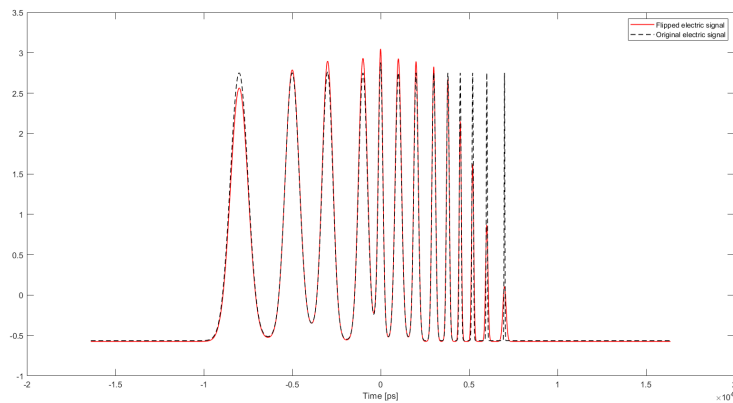Recent research in the field of telecommunications has proved the importance of achieving high bandwidth signals with the maximum achievable time as well. These ultrawide-band signals are hard to achieve through electronic means. Hence, several photonic techniques have been proposed for such purpose.

The backgroung theory of such applications has been meticulously derived; trough an exhaustive review of literature, the concept of TBWP has been reviewed and clarified by the use of some examples. Dispersion theory has been deeply studied as well in order to properly understand the employed techniques.

Among these photonic techniques, the first one to be presented has been Direct Space to Time (DST). When the conditions derived in the thesis are met, the time profile can be turned into a scaled replica of he spatial one, allowing us to modify it by changing the spatial mask applied to the outgoing pulse.

Dispersive Fourier Transformation (DFT) has also been presented. This technique is among the most used photonic techniques for AWG. In the case of DFT, also known as Frequency to time Mapping, the time profile is turned into a scaled replica of the incoming pulse frequency spectrum. Through waveshaping techniques, Direct Fourier Transformation (DFT) and photodetection, the desired MW signal can be

generated. The set-up as well as its most relevant characteristics, such as maximum achievable frequency or the TBWP have been presented. We have also derived and specified the required conditions and approximations for a proper performance of this technique, and its limits. The DFT technique presents the advantages of a simple structure, stability, as well as low losses and cost, being able to reach ultra-wide bandwidths.

The present state of the art applications of such techniques, specially of DFT, have been also described, focusing in the Time Reversal technique through photonic means, which has been demonstrated to be a very efficient solution for information transmission in wireless communications.

Finally, simulations have been performed in order to provide an idea of the numerical magnitudes of the parameters and to confirm the relevance of the techniques to practical applications, as well as their limitations. A MW signal has been firstly generated, showing alll the steps taken in the process and calculating the maximal achievable frequency and the time duration. Then, a $TBWP$=32 has been proved for a generated chirped MW signal, taking some of the results obtained in the previous simulation, in perfect agreement with the theoretical analysis. At last, we have time reversed a signal by making use of the DFT technique, showing how the bandwidth limitation affects to the reversed signal.

As further lines of research, we propose to build a set-up in the lab that may confirm the simulation results.

# References

Alexandropoulos, George C. et al. (2019). 'Indoor Time Reversal Wireless Communication: Experimental Results for Localization and Signal Coverage'. In: *ICASSP 2019 - 2019 IEEE International Conference on Acoustics, Speech and Signal Processing (ICASSP)*, pp. 7844–7848. DOI: 10.1109/ICASSP.2019.8683188 (cit. on p. 2).

Capmany, J. and Dalma Novak (June 2007). 'Microwave photonics combines two worlds'. In: *Nature Photonics* 1, pp. 319–330. DOI: 10.1038/nphoton.2007.89 (cit. on p. 1).

Chi, H. and J. Yao (2007). 'Symmetrical waveform generation based on temporal pulse shaping using amplitude-only modulator'. In: *Electronics Letters* 43, pp. 415–417 (cit. on p. 23).

Diels, Jean-Claude and Wolfgang Rudolph (2006). '1 - Fundamentals'. In: *Ultrashort Laser Pulse Phenomena (Second Edition)*. Ed. by Jean-Claude Diels and Wolfgang Rudolph. Second Edition. Burlington: Academic Press, pp. 1–60. ISBN: 978-0-12-215493-5. DOI: https://doi.org/10.1016/B978-012215493-5/50002-1. URL: https://www.sciencedirect.com/science/article/pii/B9780122154935500021 (cit. on p. 8).

Hämäläinen, Matti et al. (2021). 'Ultra-Wideband Radar-Based Indoor Activity Monitoring for Elderly Care'. In: *Sensors* 21.9. ISSN: 1424-8220. DOI: 10.3390/s21093158. URL: https://www.mdpi.com/1424-8220/21/9/3158 (cit. on p. 1).

Han, Y. and B. Jalali (2003). 'Photonic time-stretched analog-to-digital converter: fundamental concepts and practical considerations'. In: *Journal of Lightwave Technology* 21.12, pp. 3085–3103. DOI: 10.1109/JLT.2003.821731 (cit. on p. 32).

Han, Yan and Bahram Jalali (Aug. 2003). 'Time-bandwidth product of the photonic time-stretched analog-to-digital converter'. In: *Microwave Theory and Techniques, IEEE Transactions on* 51, pp. 1886–1892. DOI: 10.1109/TMTT.2003.814313 (cit. on p. 31).

J.M. Cabrera F.J. López, F.Agulló-López (1998). *Óptica electromagnética: vol I: Fundamentos. 2a ed.* Madrid: Addison-Wesley, Universidad Autónoma de Madrid (cit. on p. 55).

Jackson, John David (1975). *Classical electrodynamics; 2nd ed.* New York, NY: Wiley. URL: https://cds.cern.ch/record/100964 (cit. on p. 4).

Jäger, Dieter and Andreas Stöhr (Jan. 2005). 'Microwave Photonics - From Concepts to Applications'. In: (cit. on p. 1).

Ladányi, Libor, – Menkyna and Jarmila Mullerova (June 2013). 'ANALYSYS OF DISPERSION EFFECTS IN GAUSSIAN PULSES WITH THE VARIOUS CHIRP PARAMETERS'. In: (cit. on p. 11).

Landau, Lev Davidovich, Evgenii Mikhailovich Lifshitz and Lev Petrovich Pitaevskii (1984). *Electrodynamics of continuous media; 2nd ed.* Course of theoretical physics. Oxford: Butterworth. URL: https://cds.cern.ch/record/712712 (cit. on p. 55).

Leaird, D.E. and A.M. Weiner (2001). 'Femtosecond direct space-to-time pulse shaping'. In: *IEEE Journal of Quantum Electronics* 37.4, pp. 494–504. DOI: 10.1109/3.914397 (cit. on p. 17).

Leaird, Daniel (Jan. 2000). 'Direct space-to-time pulse shaping for ultrafast optical waveform generation'. In: *ETD Collection for Purdue University* (cit. on p. 20).

Lin, I.S., J.D. McKinney and A.M. Weiner (2005). 'Photonic synthesis of broadband microwave arbitrary waveforms applicable to ultra-wideband communication'. In: *IEEE Microwave and Wireless Components Letters* 15.4, pp. 226–228. DOI: 10.1109/LMWC.2005.845698 (cit. on p. 24).

'Manipulation of Ultrashort Pulses' (2009). In: *Ultrafast Optics*. John Wiley Sons, Ltd. Chap. 8, pp. 362–421. ISBN: 9780470473467. DOI: https://doi.org/10.1002/9780470473467.ch8. eprint: https://onlinelibrary.wiley.com/doi/pdf/10.1002/9780470473467.ch8. URL: https://onlinelibrary.wiley.com/doi/abs/10.1002/9780470473467.ch8 (cit. on p. 16).

Mei, Yuan, Boyu Xu et al. (Sept. 2016). 'Harmonics analysis of the photonic time stretch system'. In: *Appl. Opt.* 55.26, pp. 7222–7228. DOI: 10.1364/AO.55.007222. URL: http://ao.osa.org/abstract.cfm?URI=ao-55-26-7222 (cit. on p. 32).

Mei, Yuan, Yuxiao Xu et al. (2015). 'Time-bandwidth product of photonically generated wideband microwave signals based on frequency-to-time mapping'. In: *2015 Opto-Electronics and Communications Conference (OECC)*, pp. 1–2. DOI: 10.1109/OECC.2015.7340306 (cit. on p. 26).

Nahar, Niru and Roberto Rojas (Dec. 2008). 'Coupling Loss From Free Space to Large Mode Area Photonic Crystal Fibers'. In: *Lightwave Technology, Journal of* 26, pp. 3669–3676. DOI: 10.1109/JLT.2008.925034 (cit. on p. 20).

Oestges, Claude (Oct. 2004). 'Time Reversal Techniques for Broadband Wireless Communication Systems'. In: DOI: 10.13140/2.1.4635.3286 (cit. on p. 28).

Pan, Shilong and Yamei Zhang (2020). 'Microwave Photonic Radars'. In: *Journal of Lightwave Technology* 38.19, pp. 5450–5484. DOI: 10.1109/JLT.2020.2993166 (cit. on p. 1).

Papoulis, A. (1977). *Signal Analysis*. New York: McGraw-Hill (cit. on p. 12).

Qiu, R. C. et al. (2006). 'Time Reversal With MISO for Ultrawideband Communications: Experimental Results'. In: *IEEE Antennas and Wireless Propagation Letters* 5, pp. 269–273. DOI: 10.1109/LAWP.2006.875888 (cit. on p. 28).

Qiu, R.C., H. Liu and X. Shen (2005). 'Ultra-wideband for multiple access communications'. In: *IEEE Communications Magazine* 43.2, pp. 80–87. DOI: 10.1109/MCOM.2005.1391505 (cit. on pp. 1, 2).

Qiu, R.C., J.Q. Zhang and Nan Guo (2006). 'Detection of physics-based ultra-wideband signals using generalized RAKE with multiuser detection (MUD) and time-reversal mirror'. In: *IEEE Journal on Selected Areas in Communications* 24.4, pp. 724–730. DOI: 10.1109/JSAC.2005.863813 (cit. on p. 28).

Rashidinejad, Amir and Andrew M. Weiner (2014). 'Photonic Radio-Frequency Arbitrary Waveform Generation With Maximal Time-Bandwidth Product Capability'. In: *Journal of Lightwave Technology* 32.20, pp. 3383–3393. DOI: 10.1109/JLT.2014.2331491 (cit. on pp. 2, 25, 27).

Sazonov, S (June 2017). 'On the approximations of slowly varying envelope and slowly varying profile in nonlinear optics'. In: *Journal of Physics: Conference Series* 859, p. 012015. DOI: 10.1088/1742-6596/859/1/012015 (cit. on p. 8).

Solli, D., J. Chou and Bahram Jalali (Dec. 2007). 'Amplified wavelength–time transformation for real-time spectroscopy'. In: *Nature Photonics* 2, pp. 48–51. DOI: 10.1038/nphoton.2007.253 (cit. on pp. 21, 22).

Torres-Company, Victor, Daniel E. Leaird and Andrew M. Weiner (Nov. 2011). 'Dispersion requirements in coherent frequency-to-time mapping'. In: *Opt. Express* 19.24, pp. 24718–24729. DOI: 10.1364/OE.19.024718. URL: http://www.opticsexpress.org/abstract.cfm?URI=oe-19-24-24718 (cit. on p. 22).

Treacy, E. (1969). 'Optical pulse compression with diffraction gratings'. In: *IEEE Journal of Quantum Electronics* 5.9, pp. 454–458. DOI: 10.1109/JQE.1969.1076303 (cit. on p. 15).

Veli, Muhammed et al. (Jan. 2021). 'Terahertz pulse shaping using diffractive surfaces'. In: *Nature Communications* 12. DOI: 10.1038/s41467-020-20268-z (cit. on p. 1).

Wang, Chao (Dec. 2014). 'Dispersive Fourier Transformation for Versatile Microwave Photonics Applications'. In: *Photonics* 1, pp. 586–612. DOI: 10.3390/photonics1040586 (cit. on pp. 1, 22).

Wang, Chao, Hao Chi and Jianping Yao (2008). 'Photonic generation and processing of millimeter-wave arbitrary waveforms'. In: *LEOS 2008 - 21st Annual Meeting of the IEEE Lasers and Electro-Optics Society*, pp. 346–347. DOI: `10.1109/LEOS.2008.4688632` (cit. on p. 1).

Wang, Chao and Jianping Yao (2012). 'High-resolution microwave frequency measurement based on temporal channelization using a mode-locked laser'. In: *2012 IEEE/MTT-S International Microwave Symposium Digest*, pp. 1–3. DOI: `10.1109/MWSYM.2012.6259440` (cit. on p. 22).

Wang, Zhipeng et al. (2019). 'Full Analog Broadband Time-Reversal Module for Ultra-Wideband Communication System'. In: *IEEE Photonics Journal* 11.5, pp. 1–10. DOI: `10.1109/JPHOT.2019.2936501` (cit. on pp. 28, 31).

Yao, Jianping (2011). 'Photonic generation of microwave arbitrary waveforms'. In: *Optics Communications* 284.15. Special Issue on Optical Pulse Shaping, Arbitrary Waveform Generation, and Pulse Characterization, pp. 3723–3736. ISSN: 0030-4018. DOI: `https://doi.org/10.1016/j.optcom.2011.02.069`. URL: `https://www.sciencedirect.com/science/article/pii/S0030401811002549` (cit. on p. 1).

Zhang, Jiejun and Jianping Yao (2015). 'Broadband and Precise Microwave Time Reversal Using a Single Linearly Chirped Fiber Bragg Grating'. In: *IEEE Transactions on Microwave Theory and Techniques* 63.7, pp. 2166–2172. DOI: `10.1109/TMTT.2015.2432016` (cit. on pp. 29, 31).

– (2016). 'A Microwave Photonic Signal Processor for Arbitrary Microwave Waveform Generation and Pulse Compression'. In: *Journal of Lightwave Technology* 34.24, pp. 5610–5615. DOI: `10.1109/JLT.2016.2619159` (cit. on p. 22).

# Appendix A
# Maxwell Macroscopic Equations

In order to study the effect of a dispersive medium we will begin our derivation from the famous Maxwell's equations for microscopic media, presented here once again:

$$\nabla \cdot \mathbf{e} = \frac{\rho}{\epsilon_0} \qquad\qquad \nabla \times \mathbf{e} = -\frac{\partial \mathbf{b}}{\partial t} \qquad\qquad (A.1)$$

$$\nabla \cdot \mathbf{b} = 0 \qquad\qquad \nabla \times \mathbf{b} = \mu_0 \mathbf{j} + \mu_0 \epsilon_0 \frac{\partial \mathbf{e}}{\partial t} \qquad\qquad (A.2)$$

Where all is written in lowercase letters as the fields and currents are referred to the microscopic level. $\mu_0$ is the magnetic permeability of free space and $\epsilon_0$ the vacuum permittivity (also called dielectric constant). $\mathbf{e}$ is the microscopic electric field, $\mathbf{b}$ the microscopic magnetic field or flux density, $\mathbf{j}$ the electric flux and $\rho$ the charge density. However, analyzing the propagation of waves inside dense materials with these equations becomes almost impossible and not practical, since the microscopic fields that vary rapidly in space and time are not measurable. Therefore, following the procedure used by H.A.Lorentz we will go from these expressions for the microscopic fields to the ones for the macroscopic field, doing some plausible suppositions. We will define the macroscopic field as the mean of the field inside a volume.

$$\mathbf{E}(\mathbf{r}, t) = \overline{\mathbf{e}(\mathbf{r'}, t)} = \frac{1}{\Delta V} \int_{\Delta V} \mathbf{e}(\mathbf{r'}, t) dV' \qquad\qquad (A.3)$$

The charge and current can also be averaged giving place to $\rho_{macro} = \bar{\rho}$, from now on just referred as $\rho$ and $\mathbf{J} = \bar{\mathbf{j}}$. Therefore, the equations (A.1) and (A.2) can be rewritten for the macroscopic fields as:

$$\nabla \cdot \mathbf{E} = \frac{\rho}{\epsilon_0} \qquad\qquad \nabla \times \mathbf{E} = -\frac{\partial \mathbf{B}}{\partial t} \qquad\qquad (A.4)$$

$$\nabla \cdot \mathbf{B} = 0 \qquad\qquad \nabla \times \mathbf{B} = \mu_0 \mathbf{J} + \mu_0 \epsilon_0 \frac{\partial \mathbf{E}}{\partial t} \qquad\qquad (A.5)$$

Nevertheless, for better understanding of the role played by the medium in these equations we can divide the charge into free charge and bound charge, the first one referring to electrons which are freely to move in the medium and the second one to

electrons "bounded" to the positively charged nucleus. Therefore we can also divide the current into free and bound current(or flux). These relations are expressed as:

$$\rho = \rho_{free} + \rho_{bound} \qquad\qquad \mathbf{J} = \mathbf{J}_{free} + \mathbf{J}_{bound} \qquad\qquad (A.6)$$

From now one we will refer to $\rho_{free}$ and $J_{free}$ as $\rho_f$ and $J_f$ respectively and to $\rho_{bound}$ and $J_{bound}$ as $\rho_b$ and $J_b$ for simplicity. Taking these into account we can define this bound charge and current through some auxiliary measurable magnitudes (Landau, Lifshitz and Pitaevskii, 1984) as:

$$\rho_{bound} = -\nabla \cdot \mathbf{P} \qquad\qquad (A.7)$$

$$\mathbf{J}_{bound} = \frac{\partial \mathbf{P}}{\partial t} + \nabla \times \mathbf{M} \qquad\qquad (A.8)$$

Where $\mathbf{P}$ is defined as the polarization vector and $\mathbf{M}$ as the magnetization vector. As it can be seen from the previous equations, the bound charge is conserved:

$$\nabla \cdot \mathbf{J} + \frac{\partial \rho_{bound}}{\partial t} = 0 \qquad\qquad (A.9)$$

Now we can rewrite equations (A.4) and (A.5) making use of new macroscopic fields called electric displacement field $\mathbf{D}$ and the new magnetic field $\mathbf{H}$ (J.M. Cabrera, 1998).

$$\mathbf{D} = \epsilon_0 \mathbf{E} + \mathbf{P} \qquad\qquad \mathbf{H} = \frac{\mathbf{B}}{\mu_0} - \mathbf{M} \qquad\qquad (A.10)$$

To finally obtain:

$$\nabla \cdot \mathbf{D} = \rho_{free} \qquad\qquad \nabla \times \mathbf{E} = -\frac{\partial \mathbf{B}}{\partial t} \qquad\qquad (A.11)$$

$$\nabla \cdot \mathbf{B} = 0 \qquad\qquad \nabla \times \mathbf{H} = \frac{\partial \mathbf{D}}{\partial t} + \mathbf{J}_{free} \qquad\qquad (A.12)$$

Arriving to the famous Maxwell equations for the macroscopic field.

# Appendix B
# Glossary

We present the acronyms used in the thesis.

**DST**: Direct Space to Time.

**DFT**: Direct Fourier Transformation.

**TBWP**: Time Bandwidth Product.

**DST**: Direct Space to Time.

**MW**: Microwave.

**RF**: Radiofrequency.

**FTM**: Frequency to Time Mapping.

**TR**: Time Reversal.

**GVD**: Group Velocity Dispersion.

**GDD**: Group Delay Dispersion.

**GDD**: Group Delay Dispersion.

**FWHM**: Full Width at Half Maximum.

**MLL**: Mode-Locked Laser.

**SLM**: Spatial Light Modulator.

**PD**: Photodetector.

**DF**: Dispersive Fiber.

**WS**: Wave-Shaper.

**LCFBG**: Linearly Chirped Fiber Bragg Grating.

**BW**: Bandwidth.

**AWG**: Arbitrary Waveform Generation.